NON-RELATIVISTIC EFFECTIVE THEORY FOR QUARKONIUM PRODUCTION IN HADRON COLLISIONS

Martin Beneke
Theory Division, CERN
CH – 1211 Genève 23, Switzerland

ABSTRACT

I review recent progress in understanding inclusive quarkonium production in hadron collisions. The first part focuses on non-relativistic QCD as an effective theory. I discuss its differences from and similarities with effective theories describing bound states of a single heavy quark, as far as matching calculations beyond tree-level and power counting are concerned. The second part summarizes predictions for charmonium and bottomonium production at collider and fixed target experiments and their comparison with data. The emphasis here is on novel signatures due to color octet production, polarization of quarkonia and the χ_1/χ_2 ratio in fixed target collisions.

1 Introduction

The discovery of charmonium bound states[1] opened the world of heavy flavours, its wonderful variety and complexity. Since then, the focus has shifted to decays of bound states of a single heavy quark, their implications for CP violation and, perhaps, 'New Physics'. Quarkonia, due to their leptonic decay signature, on the other hand have become important tagging modes in hadron collisions and may become so for the quark-gluon plasma phase. For a theorist, therefore, the interest in quarkonia is mostly of intrinsic nature. The experimental data are there, and we are challenged to explain them.

Quarkonia are the 'atoms' of the strong force. If their Rydberg energy were larger than Λ, the dynamical low-energy scale of the strong interaction, quarkonia would be weakly coupled bound states of a heavy quark and antiquark, tractable in perturbation theory just as positronium is in electrodynamics. Neither charm nor bottom quarks are heavy enough to satisfy this requirement. And the top quark decays so rapidly that toponium has barely time to form. The binding of charmonia and bottomonia must be described non-perturbatively. Once the simplicity of a Coulombic bound state is foregone, having two heavy quarks to bind rather than a heavy and a light quark adds complications. Apart from the mass scale m_Q, set by the mass of the heavy quark, a quarkonium bound state involves three essential 'small' (compared to m_Q) scales: $m_Q v$, the typical three-momentum of the constituents in the quarkonium rest frame or the inverse quarkonium size; $m_Q v^2$, the scale of binding energies and Λ. In a heavy-light meson, there is no other dimensionless ratio of scales besides Λ/m_Q. Although none of the non-perturbative properties of quarkonia are calculated in the approach described in the sequel, the multitude of low-energy scales entails more complicated power counting rules than those applicable to heavy-light mesons. One may envisage different power counting schemes, depending on the relation of the low energy scales.

The success of non-relativistic potential models in describing static properties of the charmonium and bottomonium family suggests that these states are indeed non-relativistic and that v^2 could be used as a parameter for systematically expanding about the non-relativistic limit. With v^2 being small, quarkonium production involves two different time scales: the scale $1/m_Q$ on which a $Q\bar{Q}$ pair

is produced* and the scale $1/(m_Q v^2)$ on which the heavy quark pair binds into a quarkonium. Provided that the two stages of the production process can be separated and assuming that perturbation theory is valid at the scale m_Q, the heavy quark production part could be computed perturbatively; anything related to quarkonium formation could then be factorized into quarkonium-specific, but production process-independent, non-perturbative parameters.

A systematic realization of these ideas has been developed by Bodwin, Braaten and Lepage.[2] It is based on an effective field theory, called non-relativistic QCD (NRQCD), combined with the methods of perturbative factorization and provides us with a tool to calculate inclusive quarkonium production cross sections as a double expansion in α_s and v^2, and to leading order in Λ/m_Q in production processes with (light) hadrons in the initial state. This development is summarized in Sect. 2.

For phenomenology the most important insight[3] following from the NRQCD description of quarkonium production is that relativistic effects are very large in the production of ${}^3S_1$ states. Because v^2 is not very small, the radiation of gluons at late times in the production process, when the $Q\bar{Q}$ pair has already expanded to the quarkonium size, turns out to be favored as compared to the radiation from an almost point-like $Q\bar{Q}$ pair. As a consequence, the $Q\bar{Q}$ pair can remain in a color octet state at distances of order $1/m_Q$, a possibility that is ignored in the earlier color singlet model. The importance of these color octet contributions is supported by the large direct J/ψ and ψ' cross sections observed in $p\bar{p}$ collisions at the Tevatron.[4]

Subsequent to this initial success, almost all quarkonium production processes have been reconsidered in the light of NRQCD. The coverage of all production processes is beyond the scope of this presentation and I am restricting myself to an overview of the current status of inclusive quarkonium production at colliders and fixed target in Sects. 3 and 4, respectively. A discussion of other interesting production processes, such as photoproduction, e^+e^- annihilation, Z^0 or B decay, together with a (by now incomplete) list of references can be found in Refs.[5–7]. There is also an increasing interest in polarization phenomena, as quarkonium polarization provides a calculable in NRQCD, and sometimes striking signature

*The scale $1/m_Q$ need not appear if the quarkonium is produced through a weak interaction. Compare $B \to J/\psi X$ mediated by a $b \to c\bar{c}s$ transition with $B_c \to J/\psi X$ mediated by a $b \to c\bar{u}d$ transition. In the latter case, the $c\bar{c}$ pair is produced at distances of order of the B_c radius.

of color octet production. I believe that although the above choice of production processes is selective, it covers, on the one hand, the most dramatic new production mechanisms, and on the other hand illustrates the difficulties connected with a quantitative confirmation of the universality of long-distance parameters, as assumed in NRQCD. Especially for charmonium production, quarkonium binding effects that are at the center of tests of NRQCD factorization can rarely be exhibited in isolation from other QCD effects that reside in the short-distance part or are neglected, such as small-x and soft gluon effects (colliders, photoproduction), BFKL-type situations (photoproduction, $z \to z_{\rm max} \approx 1$), higher-twist effects (fixed target, photoproduction), and parton-hadron duality (B decay). Everything taken together makes for an intricate combination of QCD phenomena. Beyond any doubt, NRQCD is the correct theory for quarkonium systems in the heavy quark limit. Whether the charm quark mass is large enough to justify an expansion around this limit, will be decided by confronting predictions with experiments. As of now, we are only beginning to assess theoretical uncertainties and to sort out those observables that eventually will stand as solid tests of NRQCD.

2 Effective theory and factorization in quarkonium production

2.1 Non-Relativistic QCD

Let me assume that indeed $m_Q \gg m_Q v, m_Q v^2, \Lambda$. In this situation of well-separated scales, it is intuitive that a quarkonium production cross section should factorize into the production cross section of a $Q\bar{Q}$ pair times the probability that this $Q\bar{Q}$ pair forms a specific quarkonium state.

To make the scale separation explicit, one may think of integrating out all high momentum modes in the path integral down to a factorization scale μ in between m_Q and $m_Q v$. The result would be an effective action, which is highly non-local on distances $1/m_Q$. But since the low momentum modes that dominate a quarkonium bound state can not resolve such small distances, this effective action could be expanded in an infinite series of local interactions. This expansion would realize an expansion in v^2; to all orders, it would be exactly equivalent to QCD. In practice, this procedure can be carried out only in very simplified situations.

However, as long as the strong coupling α_s is small enough at the scale μ, the effective Lagrangian can be constructed perturbatively to a specified accuracy.

First, one identifies the low-energy degrees of freedom. In the non-relativistic limit, intermediate states (in the sense of time-ordered perturbation theory) containing heavy quark pairs are suppressed and integrated out. The heavy quark field Q splits into a two-spinor quark field ψ and a two-spinor antiquark field χ. The effective Lagrangian a priori consists of the most general Lagrangian, including non-renormalizable operators, consistent with the symmetries of QCD [†]. The coefficients of the operators are then tuned to reproduce QCD by comparing on-shell Green functions computed in QCD with those computed with the NRQCD Lagrangian. The desired accuracy and the values of $\alpha_s(\mu)$ and v^2 determine which operators have to be kept in NRQCD and to what loop-order the comparison has to be done. Note that since the 'matching' is carried out at a scale much above the bound state scales, only scattering diagrams have to be computed. By construction, the NRQCD Lagrangian already has the same infrared behaviour as QCD. This implies in particular that the result of matching is independent of how the small scales $m_Q v$, $m_Q v^2$ and Λ are related. However, their relation does have some consequences for which operators have to kept in NRQCD to achieve the desired accuracy.

Non-relativistic effective theory has first been introduced by Caswell and Lepage[8] as a tool to manage bound state calculations in QED. This application is particularly transparent, as both the short-distance matching and the long-distance contributions can be calculated perturbatively. The main advantage of non-relativistic QED compared to the Bethe-Salpeter approach is that the physics above the scale m_e is encoded once and forever in the effective Lagrangian. Because NRQED still contains two scales, $m_e\alpha$ and $m_e\alpha^2$, the scale separation is still not complete, but separating m_e already entails great simplifications. See Ref.[9] for a state-of-the-art calculation in NRQED.

The NRQCD Lagrangian takes the form

$$\mathcal{L}_{\rm NRQCD} = \mathcal{L}_2 + \mathcal{L}_4 + \mathcal{L}_{glue} + \ldots . \qquad (1)$$

[†]The NRQCD Lagrangian is usually written in the heavy quark rest frame and is therefore constrained only by rotational symmetry. Of course, the result of any calculation is Lorentz invariant. The 'hidden' full Lorentz symmetry constrains some of the coefficient functions in the Lagrangian.

The light quark and gluon part of the QCD Lagrangian remains unaltered and is not indicated. The contribution to the effective Lagrangian that involves two heavy quark fields can be obtained at tree-level from a Foldy-Wouthuysen-Tani transformation, generalized to the non-abelian case (see e.g. Ref.[10]):

$$\begin{aligned}\mathcal{L}_2 &= \psi^\dagger \left[iD_0 + \frac{\vec{D}^2}{2m_Q} \right] \psi + \frac{1}{8m_Q^3} \psi^\dagger \vec{D}^4 \psi + \frac{c_1}{2m_Q} \psi^\dagger \vec{\sigma} \cdot g\vec{B} \psi \\ &\quad + \frac{c_2}{8m_Q^2} \psi^\dagger (\vec{D} \cdot g\vec{E} - g\vec{E} \cdot \vec{D}) \psi + \frac{c_3}{8m_Q^2} \psi^\dagger (i\vec{D} \times g\vec{E} - g\vec{E} \times i\vec{D}) \psi \\ &\quad + \ldots + \text{charge-conjugated for the antiquark.}\end{aligned} \tag{2}$$

The leading term in square brackets describes a non-relativistic Schrödinger field theory. To reproduce the on-shell Green functions in QCD at order v^2, the four subsequent terms have to be included. Radiative corrections due to hard gluons shift their coefficients away from their tree level values $c_i = 1$. The ellipses stand for higher order terms in v^2. To reproduce Green functions with $2n$ external heavy quark fields, NRQCD must contain local operators with $2n$ quark fields. In the following, only operators with four quark fields are of interest. The generic form of $\mathcal{L}_4$ is

$$\begin{aligned}\mathcal{L}_4 &= \sum_i \frac{d_i}{m_Q^2} (\psi^\dagger \kappa_i \chi)(\chi^\dagger \kappa_i' \psi) \\ &\quad + \text{four quark scattering operators,}\end{aligned} \tag{3}$$

where κ_i (κ_i') is a matrix in spin and colour indices and may also contain factors of spatial derivatives $\vec{D}/m_Q$ in case of higher-dimension operators. The coefficients d_i of the annihilation operators are complex. Their imaginary parts describe the annihilation decay of quarkonium states.[2] Finally, integrating out heavy quark loops leads to higher-dimension operators in gluon fields, $\mathcal{L}_{glue}$, the non-abelian analogue of the Euler-Heisenberg effective Lagrangian.

The NRQCD Lagrangian $\mathcal{L}_2 + \mathcal{L}_{glue}$ coincides with the Lagrangian of heavy quark effective theory (HQET).[11] Nevertheless, the two effective theories are different, because their power counting schemes are different. Because Λ is the only low-energy scale in heavy-light mesons, the importance of operators in the HQET Lagrangian is ordered strictly by dimension. Consequently, the kinetic energy operator $\psi^\dagger \vec{D}^2/(2m_Q)\psi$ is suppressed by Λ/m_Q and the leading effective Lagrangian $\psi^\dagger iD_0 \psi$ describes a static quark. In a non-relativistic bound state we expect $\vec{D} \sim m_Q v$, but $D_0 \sim m_Q v^2$ and the kinetic term can not be neglected. A

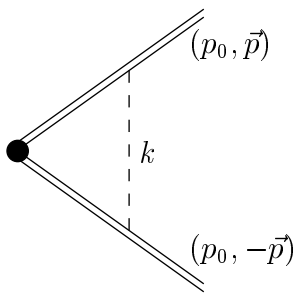

Figure 1: Coulomb correction to point-like $\psi^\dagger\chi$ creation.

more compelling argument arises, if one begins to compute Green functions in the quark-antiquark sector of NRQCD. In the following I will implicitly assume the Coulomb gauge, which makes the physics of non-relativistic bound states most transparent. The amplitude for a $Q\bar{Q}$ pair created in a point and then interacting through exchange of a Coulomb gluon (see Fig. 1), the '00'-component of the gluon propagator in this gauge, is given by

$$I = iC_F g_s^2 \int \frac{d^4k}{(2\pi)^4} \frac{1}{\vec{k}^2} \frac{1}{\left[p_0 + k_0 - \frac{(\vec{p}+\vec{k})^2}{2m_Q} + i\epsilon\right]} \frac{1}{\left[-p_0 + k_0 + \frac{(\vec{p}+\vec{k})^2}{2m_Q} - i\epsilon\right]}. \qquad (4)$$

On-shell $p_0 = \vec{p}^2/(2m_Q)$. The integral is done most easily by closing the contour in the complex k_0-plane and picking up the residues of the enclosed poles. The poles are located at $k_0 = p_0 - (\vec{p}+\vec{k})^2/(2m_Q) + i\epsilon$ and $k_0 = -p_0 + (\vec{p}+\vec{k})^2/(2m_Q) - i\epsilon$, one on each side of the real axis. Then

$$I = C_F g_s^2 \int \frac{d^3k}{(2\pi)^3} \frac{m_Q}{\vec{k}^2(\vec{k}^2 + 2\vec{p}\cdot\vec{k} - i\epsilon)} = \frac{C_F \pi \alpha_s}{4} \frac{m_Q}{|\vec{p}|} + \text{ imaginary.} \qquad (5)$$

The imaginary part is divergent and related to the Coulomb phase; the real part exhibits the well-known Coulomb divergence close to threshold.

In the static approximation, the 'kinetic term' in the propagators in (4) would be dropped and the on-shell condition reads $p_0 = 0$. In this limit the integration contour becomes pinched between the two poles and the integral becomes ill-defined. Thus, the kinetic term must be kept in the propagator to regulate the pinch-singularity. If one of the quarks were light, as in physical processes to which HQET applies, the static limit can be taken. Although the static propagator pole lies on the real axis, the contour can be deformed away from the pole.

From (5) it follows that the effective coupling for the exchange of Coulomb gluons is $\alpha_s m_Q/|\vec{p}|$. At small momenta $|\vec{p}| \sim m_Q \alpha_s$, Coulomb exchange can not be treated as a perturbation, even at weak coupling α_s. The result of resumming Coulomb gluons is of course well-known and leads to Coulomb bound state poles in the quark Green function. On the other hand, HQET contains only strongly-coupled bound states. Note that, for the purpose of matching, it is sufficient to use free NRQCD propagators. Being of infrared origin, the Coulomb-enhanced terms cancel in the matching coefficients at every order. The integral in (5) contains only one scale $|\vec{p}| = m_Q v$. Thus, its finite real part is dominated by gluons with momenta $m_Q v$ [‡].

Because the leading order Lagrangian contains m_Q in NRQCD, NRQCD does not lead to flavour symmetry. The non-perturbative properties of charmonia and bottomonia remain unrelated even in the non-relativistic limit. On the other hand, the NRQCD Lagrangian exhibits heavy-quark spin symmetry at leading order in v^2, which turns out to be useful to reduce the number of non-perturbative parameters that describe quarkonium binding.

I started out with quarkonium production, but the effective Lagrangian above does not yet allow quarkonia to be produced. One could not have expected that, because the short-distance part of a production process depends on the initial particles (hadrons, photons, Z bosons ...) that initiate it. But for every production process, the separation of short and long distances can be performed in the same way as for the effective Lagrangian above. I will elaborate on this in the following subsection.

At this point, let me pause for a discussion of the scales m_Q, $m_Q v$ and $m_Q v^2$ in charmonium and bottomonium systems. They are shown in Tab. 1, together with those for positronium for comparison. The values of v^2 are based on potential models, which describe the spectrum of quarkonia reasonably accurately. For positronium $v \sim \alpha$. In a quantum field theoretic context, v^2 could be defined as the expectation value of a derivative operator that scales like v^2 according to the scaling rules to be described later. In general, v^2 will be a complicated function of m_Q and Λ. In the limit $m_Q \to \infty$, the binding becomes Coulombic and $v \sim 1/\ln(m_Q/\Lambda)$. Neither charmonia nor bottomonia are Coulombic, because the energy scale $m_Q v^2$ is of order Λ for both quarkonium families. The same

[‡] However, they can not be thought of as on-shell intermediate states in time-ordered perturbation theory and in this sense they are not 'dynamical'.

	$c\bar{c}$	$b\bar{b}$	e^+e^-
m_Q	1.5 GeV	5 GeV	0.5 MeV
$m_Q v$	750 MeV	1.4 GeV	3.7 keV
$m_Q v^2$	400 MeV	400 MeV	25 eV
v^2	0.25	0.08	$5 \cdot 10^{-5}$
$\alpha(m_Q)/\pi$	0.1	0.07	$2 \cdot 10^{-3}$

Table 1: Scales in onium systems and the expansion parameters of the non-relativistic approximation.

conclusion can be obtained from the observation that with $r \sim 1/(m_Q v)$, the contribution of the linear term in the Cornell potential[12]

$$V(r) = -\frac{C_F \alpha_s(m_Q)}{r} + a^2 r \tag{6}$$

is non-negligible with respect to the Coulomb term. (The string tension is $a \approx 430\,\mathrm{MeV}$ and $C_F = 4/3$.) Let me stress that NRQCD does not rely in any way on a Coulombic system. It is enough that m_Q is large compared to all bound state scales. The values in Tab. 1 should be understood for the ground state of each family. Excited states are more non-relativistic and at the same time even less Coulombic. It is possible that the hierarchy of $m_Q v$ and $m_Q v^2$ with respect to Λ changes as one considers higher excited quarkonium states. Different power counting rules would then apply to different members of the onium family. Comparing the different onium systems, note that relativistic corrections (governed by the parameter v^2) are exceedingly small for positronium, comparable to radiative corrections (governed by the parameter $\alpha_s(m_Q)/\pi$) for bottomonium and definitively large for charmonium.

2.2 Factorization and matching

The factorization of a quarkonium production process, suggested in Ref.[2], begins with the observation that the creation of the $Q\bar{Q}$ pair requires an energy larger than $2m_Q$ and therefore some of the propagators of the diagram are off-shell by at least m_Q^2, much larger than the typical off-shellness in a quarkonium bound state. These propagators can be 'contracted to a point', and the remainder of

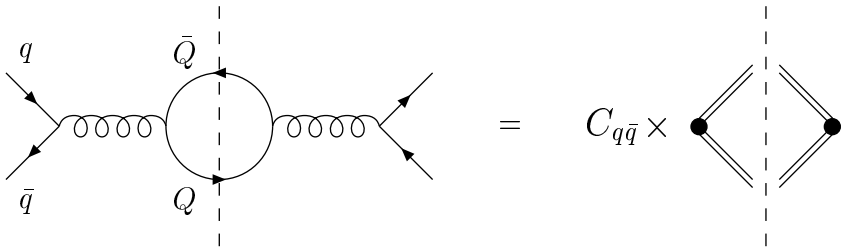

Figure 2: Trivial example of factorization.

the diagram, sensitive to distances larger than $1/m_Q$, is then associated with an operator matrix element in NRQCD. This is true, provided the production process is inclusive,

$$A + B \to \psi(P, \lambda) + X, \tag{7}$$

where X denotes light hadrons and λ the quarkonium polarization state. If it is not inclusive, the process is sensitive to the details of the hadronic final state and its long-distance contributions can not be absorbed in quarkonium-specific objects alone.

The short-distance coefficients can be computed by replacing the quarkonium in the final state by a perturbative $Q\bar{Q}$ state at small relative momentum, because the short-distance coefficient by construction does not depend on those effects that bind such a quark state into the quarkonium. Hence one can (and should) use on-shell quark states and, instead of (7), one considers

$$A + B \to Q(p)\bar{Q}(\bar{p}) + \text{gluons, light quarks}, \tag{8}$$

where

$$p = \left(\sqrt{m_Q^2 + \vec{q}_1^{\,2}}, \vec{q}_1\right) \qquad \bar{p} = \left(\sqrt{m_Q^2 + \vec{q}_2^{\,2}}, \vec{q}_2\right) \tag{9}$$

in the frame where the $Q\bar{Q}$ pair is almost at rest. (We may think of this frame as the quarkonium rest frame.) The amplitude squared is then expanded in the small quantities $\vec{q}_1$, $\vec{q}_2$ and the external heavy quark spinors are expressed in terms of two-component spinors ξ and η. For a quarkonium not at rest, one applies a Lorentz boost to the vectors p and $\bar{p}$. For the case $\vec{q}_2 = -\vec{q}_1$ explicit formulae for the reduction of the amplitude to rest frame two-spinors can be found in Ref.[13]. The simplest example of tree-level matching is shown in Fig. 2. Evaluating the

cut diagram, summing over all polarizations results in

$$\frac{16\pi^3\alpha_s^2}{27(2m_Q)^3}\,\delta(\hat{s}-4m_Q^2)\;\times\;\eta^\dagger\sigma^i T^a\xi\,\xi^\dagger\sigma^i T^a\eta + O(\vec{q}_1^{\,2},\vec{q}_2^{\,2},\vec{q}_1\cdot\vec{q}_2), \tag{10}$$

where $\hat{s}$ is the cms energy of the $q\bar{q}$ pair. The spinor product can be identified with the tree-level evaluation of the matrix element

$$\langle\mathcal{O}_8^\psi(^3S_1)\rangle \equiv \sum_{X,\lambda}\langle 0|\chi^\dagger\sigma^i T^a\psi|\psi(\lambda)+X\rangle\langle\psi(\lambda)+X|\psi^\dagger\sigma^i T^a\chi|0\rangle \tag{11}$$

where ψ is again replaced by a $Q\bar{Q}$ pair at small relative momentum. Eq. (11) displays the structure of a quarkonium production matrix element. In general, the $Q\bar{Q}$ pair can be in various color and spin states. Evidently, in our example, the $Q\bar{Q}$ pair must be in a color octet and spin-one state as expressed by the product $\sigma^i T^a$ in (11). Further terms in the expansion in $\vec{q}_1$ and $\vec{q}_2$ can be associated with operators similar in form, but with derivatives. It is natural to combine these into 'relative' and 'cms' derivatives, such that the following identifications can be made

$$\begin{aligned}(q_1-q_2)_k\;\xi^\dagger\eta \quad &\to \quad \psi^\dagger\left(i\overset{\leftrightarrow}{D}_k\right)\chi \\ (q_1+q_2)_k\;\xi^\dagger\eta \quad &\to \quad iD_k\left(\psi^\dagger\chi\right).\end{aligned} \tag{12}$$

Operators with one relative derivative on each fermion bilinear can be decomposed as ^3P_J with $J=0,1,2$. It is important that the quantum numbers of the $Q\bar{Q}$ pair in the operator need not coincide with the quantum numbers of the quarkonium ψ, because they refer to the $Q\bar{Q}$ state at a time $\tau\sim 1/m_Q$ (in the quarkonium rest frame), long before the quarkonium is formed. In between gluons with energies less than m_Q can be emitted (so that X becomes non-trivial) and change the color and spin of the $Q\bar{Q}$ pair. By the nature of factorization, these low energy gluons have to be and are included in the definition of the non-perturbative parameters above.

Operators with cms derivatives are usually neglected, because they are suppressed in v^2 according to the power counting rules discussed below[§]. These operators are important to resolve an ambiguity that arises at leading order in v^2 and which is apparent in (10): the phase space restrictions ($\hat{s}=4m_Q^2$) are expressed in terms of partonic variables, such as the quark mass, and do not reflect

[§]For quarkonium decays such operators were introduced by Mannel and Schuler.[14]

the physical phase space for a quarkonium state with mass different from $4m_Q^2$. It must be like this, because the phase space is part of the short-distance coefficient and therefore can depend only on short-distance parameters. It is also consistent, because $M_\psi - 2m_Q \sim m_Q v^2$ and the mass difference can be neglected at leading order in v^2. This negligence is certainly unjustified, if an observable is sensitive to the kinematic boundaries of phase space and leads to large ambiguities even in fully inclusive (and p_t-integrated) hadroproduction cross sections at high energies, because of the steep rise of the gluon distribution at small x. In the example of Fig. 2 $\vec{q}_1 + \vec{q}_2$ enters the phase-space delta-function. Expansion in $\vec{q}_1 + \vec{q}_2$ leads to a series of higher-dimension operators with increasingly singular coefficients, schematically written as

$$\sum_n c_n \, \delta^{(n)}(\hat{s} - 4m_Q^2) \, (\chi^\dagger \sigma^i T^a \psi) \, (\vec{D})^n \, (\psi^\dagger \sigma^i T^a \chi), \tag{13}$$

where the superscript on the delta-function denotes derivatives. The resummation of this series leads to a (non-perturbative) distribution function[15] with support properties such that its convolution with the short-distance coefficient reproduces the physical phase space constraints¶. We will meet a particular application of this in Sect. 3.1.

So far I have discussed only tree-level matching. Factorization becomes non-trivial, when one computes radiative corrections, for instance to the leading-order $q\bar{q}$ annihilation process in Fig. 2:

$$q + \bar{q} \to Q(p)\bar{Q}(\bar{p}) + g. \tag{14}$$

When the $Q\bar{Q}$ pair is in a P-wave state, the cross section is infrared divergent, when the gluon is soft.[18] (I assume that collinear singularities from emission off the initial quarks have already been absorbed into redefined partons.) For a long time, this infrared divergence has shed doubt on the perturbative calculability of P-wave quarkonium decay or production. Within the NRQCD approach, this problem finds its natural solution:[19] the infrared divergence indicates that the soft gluon emission is sensitive to bound state scales and therefore should be factored in a NRQCD matrix element. Since before gluon emission, the $Q\bar{Q}$ pair is in a color octet, spin-one state, the only candidate is $\langle \mathcal{O}_8^\psi(^3S_1) \rangle$. Indeed, since this

¶In the context of quarkonium decays, the breakdown of the NRQCD expansion near boundaries of phase space is discussed in Refs.[16,17].

matrix element appeared at leading order (Fig. 2 and (10)), a complete matching calculation includes the α_s correction to this matrix element, computed in a perturbative $Q\bar{Q}$ state at small relative momentum. This contribution is both ultraviolet and infrared divergent. The ultraviolet divergence can be absorbed into a renormalization of $\langle \mathcal{O}_8^\psi(^3S_1)\rangle$, which becomes explicitly factorization scale dependent. The infrared divergence cancels the infrared divergence in the calculation of the process (14). The short-distance coefficient of the P-wave matrix element is now infrared finite, but contains a scale-dependent $\ln(m_Q/\mu)$. The scale-dependence cancels with the scale-dependence of the octet matrix element $\langle \mathcal{O}_8^\psi(^3S_1)\rangle(\mu)$.

Note that before the advent of NRQCD, the infrared logarithm $\ln m_Q/\lambda$ was sometimes treated as an adjustable non-perturbative parameter, see for instance Ref.[20]. When this is done consistently in all production processes, this procedure is fully equivalent to taking into account the color octet contribution $\langle \mathcal{O}_8^\psi(^3S_1)\rangle$ in NRQCD. It is for this reason that the leading color octet contributions in NRQCD for P-wave production do not lead to significant differences compared to the color singlet model[21] at next-to-leading order. Ironically, color octet contributions turn out to be more important for S-wave quarkonia, precisely because they are suppressed in v^2 and not intertwined with the leading color singlet term through (logarithmic) operator mixing.

It is quite instructive to go into some details of the NRQCD part of the matching calculation. As an example, let me consider the one-loop mixing of $\langle \mathcal{O}_8^\psi(^3S_1)\rangle$ into $\langle \mathcal{O}_1^\psi(^3P_0)\rangle$. To get a non-zero contribution, a transverse gluon must be cut. The dimensions work out correctly, because a transverse gluon couples proportional to $\vec{p}/m_Q$. One of the diagrams is shown in Fig. 3; it leads to an integral

$$I = \int \frac{d^3k}{(2\pi)^3} \frac{1}{2|\vec{k}|} \frac{1}{m_Q^2} \frac{\vec{p}\cdot\vec{p}' - (\vec{p}\cdot k)(\vec{p}'\cdot k)/\vec{k}^{\,2}}{\left[|\vec{k}| - \frac{2\vec{k}\cdot\vec{p}+\vec{k}^{\,2}}{2m_Q} + i\epsilon\right]\left[|\vec{k}| - \frac{2\vec{k}\cdot\vec{p}'+\vec{k}^{\,2}}{2m_Q} + i\epsilon\right]}. \qquad (15)$$

The integral is divergent and has to be regularized. One would like to use dimensional regularization, because it makes matching calculations particularly simple. Dimensional regularization is fine, as long as the effective theory contains only one low-energy scale, such as HQET. Then all integrals in the effective theory are scaleless and vanish identically. NRQCD integrals such as (15) are not of this type.

To see how such integrals are evaluated, let me consider the following simplified

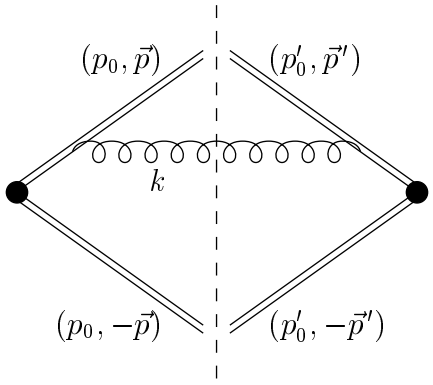

Figure 3: Contribution to mixing of $\langle \mathcal{O}_8^\psi(^3S_1)\rangle$ into $\langle \mathcal{O}_1^\psi(^3P_0)\rangle$.

version of (15), both with a cut-off and dimensional regularization:

$$J_{\Lambda_c} = \int_\lambda^{\Lambda_c} \frac{dk}{k} \frac{m_Q^2}{(m_Q + p + k)^2}$$
$$J_d = \mu^{-\epsilon} \int_\lambda^{\infty} \frac{dk}{k^{1-\epsilon}} \frac{m_Q^2}{(m_Q + p + k)^2}. \tag{16}$$

I will only consider the logarithmically divergent and finite contributions in the limit of small infrared cut-off λ. Because NRQCD is an effective theory below the scale m_Q, the ultraviolet cut-off must be chosen such that $p \ll \Lambda_c \ll m_Q$. Therefore, taking the integral J_c and expanding it in Λ_c/m_Q and p/m_Q, one gets

$$J_{\Lambda_c} = \left(1 - \frac{2p}{m_Q}\right) \ln \frac{\Lambda_c}{\lambda} - \frac{2\Lambda_c}{m_Q} + \ldots. \tag{17}$$

The same result would have been obtained, if the integrand had been first expanded in p/m_Q and k/m_Q, which are both small for $k < \Lambda_c$. Note the logarithmic term in the cut-off Λ_c, which would correspond to mixing of $\langle \mathcal{O}_8^\psi(^3S_1)\rangle$ into $\langle \mathcal{O}_1^\psi(^3P_0)\rangle$ in the real case. The dimensionally regulated integral, in the limit $\epsilon \to 0$, evaluates to

$$J_d = \frac{m_Q^2}{(m_Q + p)^2} \left(\ln \frac{m_Q + p}{\lambda} - 1\right) \tag{18}$$

and seems to have no ultraviolet divergence. The problem here is that dimensional regularization does not know about the physical requirement $p \ll \Lambda_c \ll m_Q$, that expresses that the factorization scale is smaller than m_Q, and treats the cut-off as if it were larger than m_Q. Indeed, up to power-like cut-off dependence (18)

coincides with the result for J_{Λ_c} evaluated for $\Lambda_c \gg m_Q$. We can force dimensional regularization to treat m_Q larger than all other scales by expanding the integral in m_Q before integration. The result is

$$J_d = \left(1 - \frac{2p}{m_Q}\right)\left(\frac{1}{\epsilon} - \ln\frac{\lambda}{\mu}\right) + \ldots, \tag{19}$$

in agreement with (17) up to power-like terms in the cut-off which are always zero in dimensional regularization. Thus, in dimensional regularization one must expand the integrand before integration, while with a cut-off integrating before or after expansion yields the same result, provided $\Lambda \ll m_Q$. The calculation may be simplified even further, when the infrared divergence is also regulated dimensionally. After expansion of the integrand, all integrals are scaleless and vanish in dimensional regularization. This technique has been used in Ref.[22] to obtain the NRQCD Lagrangian up to order α_s/m_Q^3 in the single heavy-quark sector.

Expanding the integrand works for matching calculations to all loops in the single heavy-quark sector, but fails in the quark-antiquark sector. Indeed, we know already from (5) that some matrix elements in the effective theory must be non-vanishing, so that the Coulomb divergence cancels in the matching. Integrands containing Coulomb singularities can not be expanded in m_Q before integration over k_0. While at one-loop it is easy to separate the Coulomb contributions explicitly, a general matching scheme based on dimensional regularization that would treat diagrams with mixed Coulomb and transverse gluon exchanges has not yet been devised. Since the problem does not appear in matching calculations with a cut-off[‖], it is not related with the effective NRQCD Lagrangian per se. See, however, Ref.[23] for an alternate view of the problem.

Summarizing the discussion of this subsection, the differential quarkonium production cross section in a hadron-hadron collision, $A + B \to \psi(P,\lambda) + X$, can be factorized as

$$d\sigma = \sum_{i,j} \int dx_1 dx_2 \, f_{i/A}(x_1) f_{j/B}(x_2) \sum_n d\hat{\sigma}_{i+j\to Q\bar{Q}[n]+X} \, \langle \mathcal{O}_n^{\psi(\lambda)} \rangle. \tag{20}$$

This equation is diagrammatically represented in Fig. 4, where I have replaced hadron B by a virtual photon for graphical simplicity. Each factor in (20) corresponds to a subgraph in Fig. 4 and a momentum scale that dominates this

[‖] NRQED calculations are naturally done in such a scheme, see e.g. Ref.[9]. Otherwise, the bound state diagrams would also have to be evaluated in dimensional regularization.

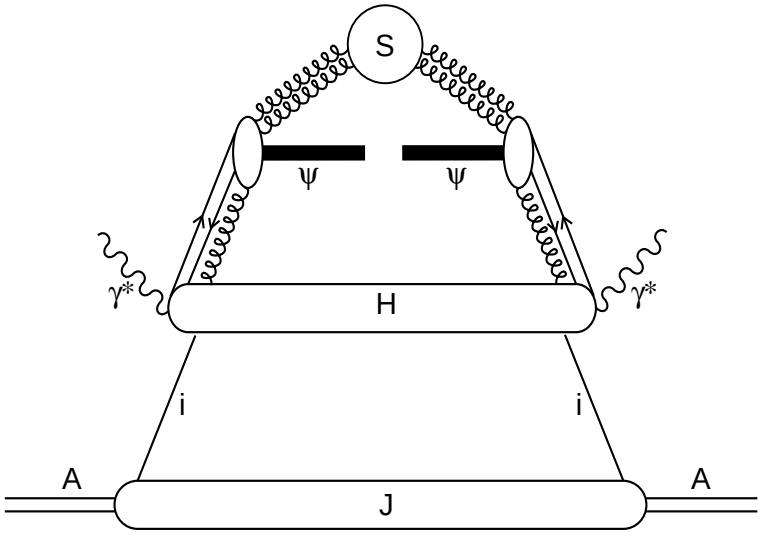

Figure 4: Diagrammatic representation of factorization in $\gamma^* + A \to \psi + X$. For the cross section the diagram has to be cut.

subgraph. The amplitude squared for $A \to i +$ remnant J is given by the parton distribution $f_{i/A}(x_1)$. The typical virtualities in this subgraph are of order Λ^2. Parton i then participates in a hard collision H, in which a $Q\bar{Q}$ pair in a certain state n is produced. This involves energies of order m_Q. The $Q\bar{Q}$ pair (and, in general, additional gluons) connects to the quarkonium subgraph, represented by the NRQCD matrix element $\langle \mathcal{O}_n^{\psi(\lambda)} \rangle$, which contains all soft lines that are sensitive to the bound state scale $m_Q v^2$. After factorizing initial state singularities into redefined parton distributions and performing the NRQCD matching as described above, the short-distance cross section $d\hat{\sigma}_{i+j\to Q\bar{Q}[n]+X}$ is infrared finite, but depends on the collinear and NRQCD factorization scale. The scale dependence cancels in the product (20).

Note that the factorization formula above implies complete factorization between final and initial state; all lines connecting both run through the hard part of the diagram. The cancellation of soft gluons, that could connect the quarkonium and remnant jet part, is believed, but not yet really proven, to hold perturbatively for inclusive quarkonium production. This is quite intuitive, if the quarkonium is scattered at large transverse momentum with respect to the colliding hadrons. It holds also for the total quarkonium production cross section even though the bulk cross section is from quarkonia at small transverse momentum. This is intuitive only in the Coulombic limit $m_Q v^2 \gg \Lambda$, in which quarkonium formation has ter-

minated long before the time-scale of a second interaction with the remnant. Since perturbative matching is insensitive to the relation of low energy scales, factorization should thus hold in perturbation theory. The calculation of next-to-leading corrections to total P-wave production cross sections[24] confirms factorization at the one-loop level. The mathematical statement of factorization is thus that all corrections to (20) scale as some power of $1/m_Q$, or another kinematic scale larger than m_Q, as $m_Q \to \infty$. (Recall that relativistic and radiative corrections scale as $1/\ln m_Q$ in this limit.) Corrections should then be suppressed as Λ divided by potentially any other scale in the process. Since $m_Q v^2 \sim \Lambda$ for charmonium and bottomonium, one may expect large 'higher-twist' corrections in fixed-target collisions, when the heavy quark-antiquark pair moves parallel with a remnant jet and remains in its hadronization region over a time $1/\Lambda$ in the quarkonium rest frame. Even if higher-twist effects scale only as Λ^2/m_c^2 for charmonium, they can be expected to be non-negligible for total cross sections.

2.3 Power counting (velocity scaling)

The factorization formula (20) contains an infinite series of non-perturbative production matrix elements $\langle \mathcal{O}_n^{\psi(\lambda)} \rangle$ and would be useless, if it could not be truncated after a finite number of terms. A first indication comes from the dimension of the operators, since any power of $1/m_Q$ in the coefficient of an operator can be compensated only by one of the low-energy scales $m_Q v$, $m_Q v^2$ or Λ. However, the matrix elements can have additional suppressions beyond their dimension, because of the particular structure of a non-relativistic bound state.

The standard power counting (or 'velocity scaling') rules are due to Ref.[25]. For example, heavy quark fields scale as $(m_Q v)^{3/2}$, because $\int d^3r\, \psi^\dagger \psi$ counts heavy quark number and $r \sim 1/|\vec{p}| \sim 1/(m_Q v)$. The Virial theorem relates the potential to the kinetic energy $E \sim m_Q v^2$ and leads to $g\vec{E} \sim m_Q^2 v^3$ for the electric field inside a quarkonium. From the equation of motion for the vector potential, $g\vec{B} \sim m_Q^2 v^4$ follows for the magnetic field. As a consequence the 'dipole interaction' $\psi^\dagger (g\vec{A} \cdot \vec{\partial}/m_Q^2)\psi$ and 'magnetic interaction' $\psi^\dagger (g\vec{B} \cdot \vec{\sigma}/(2m_Q))\psi$ in the NRQCD Lagrangian both scale as v^2 relative to the Coulomb interaction.

It follows that a matrix element such as $\langle \mathcal{O}_1^{J/\psi}(^3S_1) \rangle$ scales as v^3, because a $Q\bar{Q}$ pair in a color singlet $^3S_1$ state overlaps with the leading Fock state wavefunction

of a J/ψ without need of soft gluon emission**. In the following the scaling of all matrix elements will be considered relative to $\langle \mathcal{O}_1^{J/\psi}(^3S_1)\rangle$, that is, I put $\langle \mathcal{O}_1^{J/\psi}(^3S_1)\rangle \sim 1$. To estimate the scaling of other matrix elements, the multipole suppression of gluon emission with momentum $\vec{k} \sim m_Q v^2 \ll \vec{p} \sim m_Q v$ has to be taken account as a consequence of the two low energy scales present in NRQCD. (In the context of NRQED, the separation of photons with momenta $|\vec{k}| \sim m_e v$ and $|\vec{k}| \sim m_e v^2$ and the power counting for the two momentum regions has been analyzed in detail by Labelle.[26])

Consider the P-wave matrix element $\langle \mathcal{O}_8^{J/\psi}(^3P_0)\rangle$ in a J/ψ state. A non-zero overlap requires the emission of gluons into the final state. For a single gluon emission, one such diagram looks exactly like Fig. 3. The $Q\bar{Q}$ vertex carries a derivative for the P-wave operator and the transverse gluon also couples proportional to $\vec{p}/m_Q$ from the dipole interaction term above. Thus $\langle \mathcal{O}_8^{J/\psi}(^3P_0)\rangle$ scales as $p^4/m_Q^4 \sim v^4$ relative to $\langle \mathcal{O}_1^{J/\psi}(^3S_1)\rangle$, to which diagrams with out radiation would contribute.

Consider now $\langle \mathcal{O}_8^{J/\psi}(^1S_0)\rangle$, which requires a spin-flip transition. As the chromomagnetic interaction is proportional to the gluon momentum, a diagram such as Fig. 3 leads to (cf. (15))

$$\begin{aligned} I &= \frac{\alpha_s}{4m_Q^2}\int^{\Lambda_c}\frac{d^3k}{(2\pi)^3}\frac{1}{2|\vec{k}|}\,\frac{P_{ij}\,(\vec{k}\times\vec{\sigma})_i\,(\vec{k}\times\vec{\sigma})_j}{\left[p_0+|\vec{k}|-\frac{(\vec{p}+\vec{k})^2}{2m_Q}+i\epsilon\right]\left[p_0'+|\vec{k}|-\frac{(\vec{p}'+\vec{k})^2}{2m_Q}+i\epsilon\right]} \\ &\sim \alpha_s\frac{\Lambda_c^2}{m_Q^2} + \text{magnetic dipole contribution}, \end{aligned} \tag{21}$$

where $P_{ij} = \delta_{ij} + k_i k_j/\vec{k}^{\,2}$. In the second line I have (schematically) separated the contribution from the region $|\vec{k}| \sim m_Q v$. In this region the $|\vec{k}|$-terms in the quark propagators dominate, the integrand becomes independent of the bound state structure and results in a pure (power-like) cut-off term. The contribution from $|\vec{k}| \sim m_Q v^2$ is denoted as 'magnetic dipole' and scales as

$$\frac{\alpha_s}{m_Q^2}\,|\vec{k}|^2 \sim v^2\lambda^2 \sim v^4, \tag{22}$$

where for $|\vec{k}| \sim m_Q v^2$ the coupling α_s must be counted as 1. $\lambda \equiv k/p \sim v$ corresponds to the ratio of the size of the quarkonium and the wavelength of the

**Up to corrections in v^2, this matrix element coincides with the wavefunction at the origin squared. Keeping only this contribution, NRQCD reproduces the color singlet model for S-wave quarkonia.

	$\langle\mathcal{O}_1^\psi(^3S_1)\rangle$	$\langle\mathcal{O}_8^\psi(^3S_1)\rangle$	$\langle\mathcal{O}_8^\psi(^1S_0)\rangle$	$\langle\mathcal{O}_8^\psi(^3P_0)\rangle$
NRQCD	1	v^4	$v^2\lambda^2$	v^4
CEM	1	1	1	v^2

Table 2: Velocity scaling in NRQCD and the color evaporation model (CEM) relative to $\langle\mathcal{O}_1^\psi(^3S_1)\rangle$ for S-wave quarkonia. The 'standard' velocity counting is recovered for $\lambda = v$.

emitted gluon and provides the expansion parameter for the multipole expansion. In general, once gluons of momentum $m_Q v$ are separated, the interaction vertices of NRQCD can be multipole-expanded. This is true beyond perturbation theory and justifies the single-gluon approximation which I used for illustration. Thus $\langle\mathcal{O}_8^{J/\psi}(^1S_0)\rangle$ scales as v^4, if the cut-off term in (21) could be discarded. If one identifies $\Lambda_c \sim m_Q v$ and α_s at the scale $m_Q v$ with v, as suggested by a Coulombic limit, the cut-off term scales as[27,28] v^3. Being pure cut-off, however, it should not be taken into account to estimate the scaling of low-energy matrix elements. It would be cancelled with a contribution to the coefficient function, if it were evaluated with the same cut-off. In dimensional regularization, the contribution from $|\vec{k}| \sim m_Q v$ gives a tadpole-like integral and would be set to zero naturally.

The multipole suppression is effective as long as $m_Q v \gg \Lambda \sim m_Q v^2$ holds. If, on the other hand, $m_Q v \sim \Lambda \gg m_Q v^2$, the typical momenta of (soft) gluons would be Λ and the multipole expansion would not work, as $\lambda = 1$. We can keep λ as a free parameter and conceive an intermediate case for J/ψ or, in particular, ψ'. The power counting for the most important $Q\bar{Q}$ states is summarized in Tab. 2 and 3 for S- and P-wave quarkonia, respectively. For each $Q\bar{Q}$ state, there exist v^2 corrections due to operators with two and more derivatives on a single bilinear of fermion fields. Since their coefficient functions are not enhanced by fewer powers of α_s compared to the leading operator in each channel, I will not discuss them further. Like operators with cms derivatives, these operators can be important in specific kinematic regions.

Before closing this section, I would like to mention the color evaporation model[29] (CEM), the only remaining potential competitor of NRQCD ††. In the

††As alluded to earlier, the color singlet model has been swallowed by NRQCD and lost its justification hence after.

	$\langle \mathcal{O}_1^\psi(^3P_J)\rangle$	$\langle \mathcal{O}_8^\psi(^3S_1)\rangle$	$\langle \mathcal{O}_8^\psi(^3P_{J'})\rangle$	$\langle \mathcal{O}_8^\psi(^1P_1)\rangle$	$\langle \mathcal{O}_1^\psi(^3S_1)\rangle$	$\langle \mathcal{O}_8^\psi(^3D_{J''})\rangle$
NRQCD	v^2	v^2	v^6	$v^4\lambda^2$	v^6	v^6
CEM	v^2	1	v^2	v^2	1	v^4

Table 3: Velocity scaling in NRQCD and the color evaporation model (CEM) relative to $\langle \mathcal{O}_1^\psi(^3S_1)\rangle$ for P-wave quarkonia with total angular momentum J. The 'standard' velocity counting is recovered for $\lambda = v$.

CEM, the NRQCD expansion on the right hand side of (20) becomes replaced by an average,

$$\sum_n d\hat{\sigma}_{i+j\to Q\bar{Q}[n]+X}\,\langle \mathcal{O}_n^{\psi(\lambda)}\rangle \to f_\psi \int_{2m_Q}^{2m_{Qq}} dM\, d\hat{\sigma}_{i+j\to Q\bar{Q}(M)+X}/dM, \qquad (23)$$

i.e., the open heavy quark cross section is integrated over the invariant mass M of the $Q\bar{Q}$ pair up to the open heavy flavour threshold. It is then assumed that the quarkonium production cross section is a universal (for each ψ) fraction f_ψ of the sub-threshold cross section.

Spiritually, the CEM is close to NRQCD in that it also allows a $Q\bar{Q}$ pair in a color octet state in the hard collision to hadronize into a quarkonium. It is also clear that, because the NRQCD expansion arises from an expansion of the open $Q\bar{Q}$ production amplitude at small relative $Q\bar{Q}$ momentum and because $m_{Qq} - m_Q \ll m_Q$, the CEM is very similar to NRQCD as far as kinematic dependences of the production cross section are concerned. The difference arises in the importance that is assigned to the various terms that arise in the expansion close to threshold. In terms of NRQCD matrix elements this difference can be summarized by the statement that the power counting implied by the CEM would assign v^{2d-6} to any dimension d operator, independent of the color and spin state of the $Q\bar{Q}$ pair (see Tab. 2 and 3). The usual argument is that the emission of soft gluons in the hadronization of a $Q\bar{Q}$ pair randomizes spin and color, so that by the time the quarkonium forms, any information on the state of the initial $Q\bar{Q}$ pair has been lost. The problem with the argument is that soft gluons do not flip a heavy quark spin easily, a piece of information that is incorporated in NRQCD via spin symmetry but disregarded in the CEM. Moreover, the CEM treats a quarkonium

as if its size were that of a light hadron, in which case the multipole expansion is not valid. The CEM also does not incorporate the heavy quark limit, in which the binding becomes Coulombic. This does not impede the color evaporation model to provide a description that is phenomenologically successful in some cases, in particular as – in contrast to the color singlet model – the correct kinematic dependences are incorporated. In general, with only one parameter f_ψ the CEM is too restrictive. It predicts are universal $\chi/(J/\psi)$-ratio $f_\chi/f_{J/\psi}$, which is not supported by the comparison of quarkonium production in fixed target collisions, photoproduction and B decay. Note that – as NRQCD – the CEM is based on a leading-twist approximation to the heavy quark production cross section.

2.4 Quarkonium Polarization

NRQCD factorization also predicts the polarization of the produced quarkonia, although, in general, at the expense of introducing further non-perturbative matrix elements that do not appear in the cross section summed over all ψ polarization states ('unpolarized cross section'). Let me sketch the decomposition of matrix elements for the case of a S-wave, spin-triplet quarkonium.[30,31,13]

After expansion of the $Q\bar{Q}$ production amplitude squared in relative momentum, and after decomposing color indices into color singlet and a color octet term, and spin indices in a spin singlet and triplet term, the cross section can be written as a sum (compare with (20))

$$\sum_n C_{n;ij}(\mu)\,\langle \mathcal{O}^{\psi(\lambda)}_{n;ij}\rangle, \tag{24}$$

where the short-distance part C is still coupled to the matrix elements through three-vector indices that arise in the expansion in relative momentum. To decouple these indices, one writes down the most general decomposition of the Cartesian tensor $\langle \mathcal{O}^{\psi(\lambda)}_{n;ij}\rangle$ incorporating rotational invariance and the fact that the rest frame matrix elements can depend only on the polarization vector (in general, tensor) of the quarkonium.

The constraints from spin symmetry are incorporated as follows. Because of spin symmetry, spin and orbital angular momentum are separately good quantum numbers at leading order in the velocity expansion. The angular momentum part of the quarkonium wave function is thus a direct product $S \times L_i$ (i may be a multi-index for orbital angular momentum greater than 1) in spin and orbital angular

momentum and can be represented as

$$\begin{aligned} {}^1S_0 \qquad & 1 \\ {}^3S_1 \qquad & \epsilon_a(\lambda)\,\sigma^a \\ {}^1P_1 \qquad & \epsilon_i(\lambda) \\ {}^3P_J \qquad & \sum_{\alpha,\rho}\langle J\lambda|1\rho;1\alpha\rangle\,\epsilon_i(\rho)\epsilon_a(\alpha)\,\sigma^a \end{aligned} \tag{25}$$

in the quarkonium rest frame, where $\langle J\lambda|1\rho;1\alpha\rangle$ denotes a Clebsch-Gordon coefficient and $\epsilon(\lambda)$ an angular momentum-one polarization vector. A general NRQCD matrix element can then be written as

$$\begin{aligned} &\sum_X \langle 0|\chi^\dagger \kappa D_{i_n}\ldots D_{i_n}\psi|\psi(\lambda)+X\rangle\langle\psi(\lambda)+X|\psi^\dagger\kappa' D_{j_n}\ldots D_{j_m}\chi|0\rangle \\ &\qquad = \mathrm{tr}(\kappa S)\,\mathrm{tr}(\kappa' S)\,L_iL_j\,\xi_{iji_1\ldots i_nj_1\ldots j_m}, \end{aligned} \tag{26}$$

where κ is a matrix in spin and color indices and

$$\begin{aligned} \xi_{kl} &= a\,\delta_{kl} \\ \xi_{klmn} &= b_0\delta_{kl}\delta_{mn}+b_1\delta_{km}\delta_{ln}+b_2\delta_{kn}\delta_{lm} \end{aligned} \tag{27}$$

etc.. a, b_i are scalar non-perturbative parameters. Some of them can be expressed in terms of those that appear in unpolarized production by taking contractions or summing over polarizations. For a S-wave quarkonium, the orbital angular momentum part is trivial and its is straightforward to obtain

$$\begin{aligned} &\sum_X\langle 0|\chi^\dagger\sigma^a\psi|\psi(\lambda)+X\rangle\langle\psi(\lambda)+X|\psi^\dagger\sigma^b\chi|0\rangle = \frac{1}{3}\langle\mathcal{O}_1^\psi({}^3S_1)\rangle\,\epsilon^{a*}(\lambda)\epsilon^b(\lambda) \\ &\sum_X\langle 0|\chi^\dagger\sigma^aT^A\psi|\psi(\lambda)+X\rangle\langle\psi(\lambda)+X|\psi^\dagger\sigma^bT^a\chi|0\rangle = \frac{1}{3}\langle\mathcal{O}_8^\psi({}^3S_1)\rangle\,\epsilon^{a*}(\lambda)\epsilon^b(\lambda) \\ &\sum_X\langle 0|\chi^\dagger\sigma^aT^A\left(-\frac{i}{2}\overleftrightarrow{D}_i\right)\psi|\psi(\lambda)+X\rangle\langle\psi(\lambda)+X|\psi^\dagger\sigma^bT^A\left(-\frac{i}{2}\overleftrightarrow{D}_j\right)\chi|0\rangle \\ &\qquad = \langle\mathcal{O}_8^\psi({}^3P_0)\rangle\,\delta_{ij}\,\epsilon^{a*}(\lambda)\epsilon^b(\lambda) \\ &\sum_X\langle 0|\chi^\dagger T^A\psi|\psi(\lambda)+X\rangle\langle\psi(\lambda)+X|\psi^\dagger T^A\chi|0\rangle = \frac{1}{3}\langle\mathcal{O}_8^\psi({}^1S_0)\rangle. \end{aligned} \tag{28}$$

The matrix elements on the right hand side include implicitly a sum over polarization as in the definition of Ref.[2] and in (11). For the last line zero would be obtained in the spin-symmetry limit. The factor 1/3 here follows from rotational invariance. Note that the decomposition of P-wave operators in the third

and fourth line is not diagonal in the angular momentum basis JJ_z. As a consequence, for S-wave production, the total angular momentum of an intermediate quark pair in a P-wave state is not a good quantum number. In this basis, interference term between states with different total angular momentum have to be included to obtain a factorized form of polarized production cross sections.[30] These interference terms vanish when all polarizations are summed over.

Notice that after applying spin symmetry, no new non-perturbative matrix elements had to be introduced to describe polarized S-wave quarkonium production as compared to unpolarized production at this order in the velocity expansion. For P-wave quarkonia, this is also true at leading order in v^2, but – in contrast to S-wave states – no more for v^4 corrections.

3 Quarkonium production at the Tevatron

In this present section I discuss the comparison of predictions for S-wave production with Tevatron data,[4,32] which inspired to a large extent the theoretical development described above. In Sect. 4 fixed-target data will be revisited in the NRQCD approach.

3.1 Cross sections

Let me follow the chronology of the development of theory and data. When CDF measured, for the first time, separately J/ψ and ψ' production not coming from B decay ('prompt'), they found much larger cross sections than expected.[4] The expectation then was based on the color singlet process

$$g + g \to c\bar{c}[^3S_1^{(1)}] + g : \qquad \alpha_s^3 \frac{(4m_c^2)^2}{p_t^8} \tag{29}$$

for the direct production of S-wave states, with additional contributions to J/ψ from radiative decays of χ_{c1} and χ_{c2}. As indicated, this lowest order process leads to a very steep p_t-spectrum $d\hat{\sigma}/dp_t^2$ of the short-distance cross section. On the other hand at $p_t \gg 2m_Q$ the quarkonium mass can be considered as small and the inclusive production cross section, like any single-particle inclusive cross section in QCD, should exhibit scaling: $d\hat{\sigma}/dp_t^2 \sim 1/p_t^4$ up to logarithms. Such processes can be described by convoluting a (properly factorized) parton production cross section with a fragmentation function $D_{i\to H}(z)$, where z denotes the fraction of

i's momentum transferred to the hadron H. Braaten and Yuan[33] noted that for quarkonia the dependence of fragmentation functions on z can be calculated in the NRQCD approach. Since the hadronization of the $Q\bar{Q}$ pair takes place by emission of gluons with momenta of order $m_Q v^2$ in the quarkonium rest frame, the energy fraction of the quarkonium relative to the fragmenting parton differs from that of the $Q\bar{Q}$ pair only by an amount $\delta z \sim v^2 \ll 1$. They argued that the higher-order color singlet process

$$g + g \to \left[c\bar{c}[^3S_1^{(1)}] + gg\right] + g : \qquad \alpha_s^5 \frac{1}{p_t^4} \tag{30}$$

exceeds (29) for $p_t > 7\,\mathrm{GeV}$ as relevant to most of the Tevatron data. This expectation was born out by detailed analyses.[34] At this point, taking also into account fragmentation production of P-wave states and their subsequent decay, theory and data seemed to agree for J/ψ production, but showed a factor of 30 discrepancy in overall normalization for ψ', a discrepancy then referred to as ψ'-anomaly. The discrepancy in normalization indicated that an additional fragmentation contribution had been missed. Braaten and Fleming[3] suggested that the color octet fragmentation process

$$g + g \to c\bar{c}[^3S_1^{(8)}] + g : \qquad \alpha_s^3\, v^4\, \frac{1}{p_t^4}, \tag{31}$$

where a gluon fragments as $g \to c\bar{c}[^3S_1^{(8)}]$, could make up for the missing piece. The price to pay is a new parameter $\langle \mathcal{O}_8^{\psi'}(^3S_1)\rangle$ that had to be fitted to the data. Because (31) has two powers of α_s/π less than (30), the magnitude of $\langle \mathcal{O}_8^{\psi'}(^3S_1)\rangle$ turned out to be consistent with its v^4 suppression according to the scaling given in Tab. 2. Subsequently, CDF was able to remove χ feed-down from J/ψ production. The same discrepancy as for ψ' appeared in the J/ψ cross section and could be explained as for ψ' by color octet fragmentation.[35]

With this explanation of the ψ'-anomaly at hand, further studies focused on finding additional consistency checks of the color octet hypothesis beyond the consistent size of the octet matrix element. One such check derives from polarization and will be described in the next subsection. Others come from different charmonium production processes. Apart from fixed-target production discussed in the following section, I do not undertake such a comparison in this article, a comparison that would in any case be still preliminary. Let me instead continue with the Tevatron analysis and discuss the uncertainties in the theoretical prediction.

At moderate $p_t \sim 2m_Q$ two further octet production channels, which do not have a fragmentation interpretation at order α_s^3,

$$g + g \to c\bar{c}[{}^1S_0^{(8)}, {}^3P_J^{(8)}] + g : \qquad \alpha_s^3\, v^4\, \frac{4m_c^2}{p_t^6}, \tag{32}$$

need to be considered, too, even though they seem to be suppressed by v^4 with respect to the color singlet process (29). (I'll come back to this point later.) These contributions have been calculated in Refs.[36,37] and turn out to be significant for $p_t < 10\,\mathrm{GeV}$. In this region (and taking $m_c = 1.5\,\mathrm{GeV}$) the transverse momentum distribution is sensitive only to the combination $M_{3.5}^{\psi}({}^1S_0^{(8)}, {}^3P_0^{(8)})$ defined as

$$M_k^{\psi}({}^1S_0^{(8)}, {}^3P_0^{(8)}) \equiv \langle \mathcal{O}_8^{\psi}({}^1S_0)\rangle + \frac{k}{m_c^2}\,\langle \mathcal{O}_8^{\psi}({}^3P_0)\rangle. \tag{33}$$

This matrix element appears as a second fit parameter. The fits to the CDF data[32] are shown in Figs. 5 and 6. These fits are based on a combined fit of J/ψ and ψ' data, keeping the ratios of octet matrix elements for J/ψ and ψ' fixed. See Ref.[37] for further details. The values of the matrix elements with parameters as specified for Fig. 5 are found to be

$$\begin{aligned}
&\langle \mathcal{O}_8^{J/\psi}({}^3S_1)\rangle = 1.06 \cdot 10^{-2}\,\mathrm{GeV}^3 \\
&\langle \mathcal{O}_8^{J/\psi}({}^1S_0)\rangle + \frac{3.5}{m_c^2}\,\langle \mathcal{O}_8^{J/\psi}({}^3P_0)\rangle = 4.38 \cdot 10^{-2}\,\mathrm{GeV}^3 \\
&\langle \mathcal{O}_8^{\psi'}({}^3S_1)\rangle = 0.44 \cdot 10^{-2}\,\mathrm{GeV}^3 \\
&\langle \mathcal{O}_8^{\psi'}({}^1S_0)\rangle + \frac{3.5}{m_c^2}\,\langle \mathcal{O}_8^{\psi'}({}^3P_0)\rangle = 1.80 \cdot 10^{-2}\,\mathrm{GeV}^3.
\end{aligned} \tag{34}$$

Note that Figs. 5 and 6 include only α_s^3 processes. The leading color singlet process at large p_t, Eq. (30), is not included but would fall below the data by a factor of 30 as mentioned above.

It is not surprizing that a good fit of the data can be obtained with two contributions to the fit that scale as $1/p_t^4$ and $1/p_t^6$ at large p_t. It is not at all clear how accurate the fitted matrix elements are, however, as any effect that modifies the slope of the p_t-spectrum would affect the relative weight assigned to the two matrix elements $\langle \mathcal{O}_8^{\psi}({}^3S_1)\rangle$ and $M_{3.5}^{\psi}({}^1S_0^{(8)}, {}^3P_0^{(8)})$. Some uncertainties that enter the theoretical prediction can be enumerated:

1. One may vary the parameters of the calculation such as α_s, the renormalization and/or factorization scale, as well as the parton distribution set. A

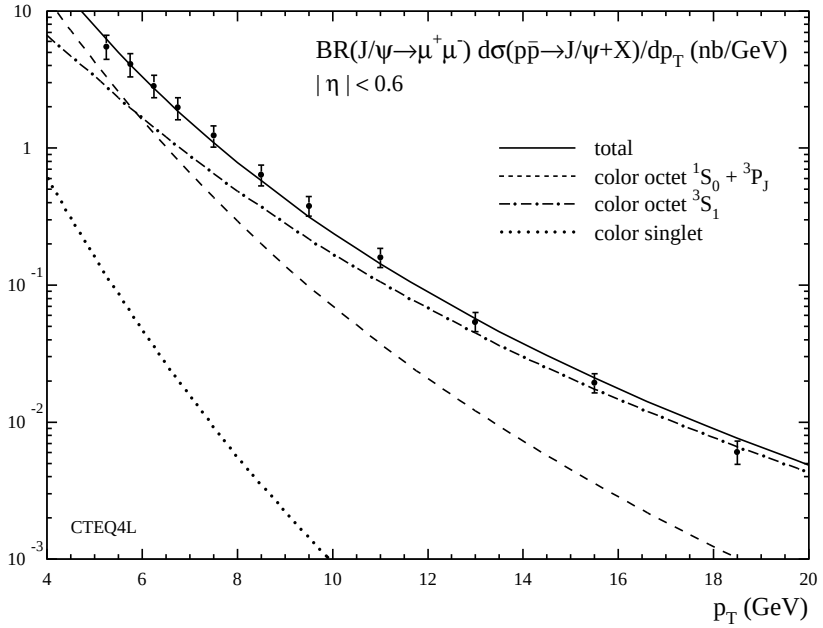

Figure 5: Fit of color octet contributions to direct J/ψ production data from CDF ($\sqrt{s} = 1.8\,\mathrm{TeV}$, pseudo-rapidity cut $|\eta| < 0.6$). Theory: CTEQ4L parton distribution functions, the corresponding $\Lambda_4 = 235\,\mathrm{MeV}$, factorization scale $\mu = (p_t^2 + 4m_c^2)^{1/2}$ and $m_c = 1.5\,\mathrm{GeV}$. Taken from Ref.[37].

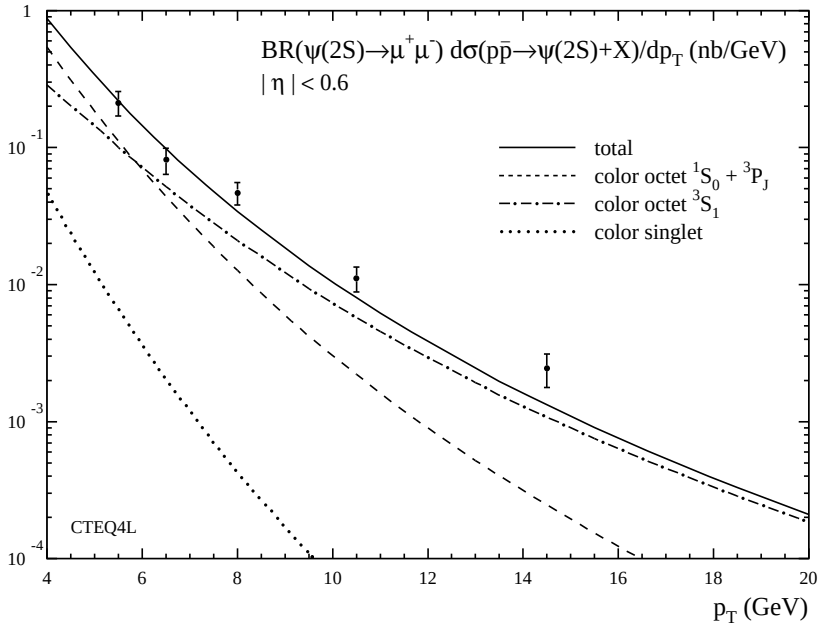

Figure 6: Same as Figure 5 for prompt ψ' production.

	CTEQ4L	GRV (1994) LO	MRS(R2)
$\langle \mathcal{O}_8^{J/\psi}(^3S_1)\rangle$	$1.06 \pm 0.14^{+1.05}_{-0.59}$	$1.12 \pm 0.14^{+0.99}_{-0.56}$	$1.40 \pm 0.22^{+1.35}_{-0.79}$
$M_{3.5}^{J/\psi}(^1S_0^{(8)},^3P_0^{(8)})$	$4.38 \pm 1.15^{+1.52}_{-0.74}$	$3.90 \pm 1.14^{+1.46}_{-1.07}$	$10.9 \pm 2.07^{+2.79}_{-1.26}$
$\langle \mathcal{O}_8^{\psi'}(^3S_1)\rangle$	$0.44 \pm 0.08^{+0.43}_{-0.24}$	$0.46 \pm 0.08^{+0.41}_{-0.23}$	$0.56 \pm 0.11^{+0.54}_{-0.32}$
$M_{3.5}^{\psi'}(^1S_0^{(8)},^3P_0^{(8)})$	$1.80 \pm 0.56^{+0.62}_{-0.30}$	$1.60 \pm 0.51^{+0.60}_{-0.44}$	$4.36 \pm 0.96^{+1.11}_{-0.50}$

Table 4: NRQCD matrix elements in $10^{-2}\,\mathrm{GeV}^3$. First error statistical, second error due to variation of scale. Ratio of ψ' to J/ψ fixed. Parton densities from Ref.[38].

different value in α_s modifies the over-all normalization and also the slope of the p_t-distribution, because the coupling is evaluated at $\mu = \sqrt{4m_c^2 + p_t^2}$.

The parametrization of the gluon density affects the prediction in a systematic way. Roughly, we may estimate the typical proton momentum fractions of the gluons that participate in the hard collision as $x_g \sim 2\sqrt{p_t^2 + 4m_c^2}/\sqrt{s}$ for a given value of p_t. A gluon density with steeper small-x behaviour therefore steepens the p_t-spectrum for the $^3S_1^{(8)}$ component. As a consequence, the $M_{3.5}^{\psi}(^1S_0^{(8)},^3P_0^{(8)})$ component whose magnitude depends crucially on the data being somewhat steeper than the $^3S_1^{(8)}$ component, decreases for a steeper gluon density.

The combined effect of a lower α_s and flatter small-x gluon distribution is clearly seen in Tab. 4 by comparing the value of $M_{3.5}^{\psi}(^1S_0^{(8)},^3P_0^{(8)})$ obtained with MRS(R2) distributions with the one obtained from CTEQ4L or GRV. In contrast, the value of $\langle \mathcal{O}_8^{J/\psi}(^3S_1)\rangle$ is rather insensitive to the parton distribution set, but absorbs most of the uncertainty in overall normalization obtained by varying the factorization scale μ within a factor two about $\sqrt{4m_c^2 + p_t^2}$ (see the second error in Tab. 4). From these variations alone one can conclude that none of the two matrix elements is determined to an accuracy better than a factor of 2 and that $M_{3.5}^{\psi}(^1S_0^{(8)},^3P_0^{(8)})$ is particularly sensitive to any effect that influence the slope of the p_t-distribution.

2. The variation of renormalization and factorization scale gives some insight into the magnitude of higher-order corrections in α_s only for those contributions that have the same kinematic dependence as the leading-order term. In high-energy processes or at not so large transverse momentum this may be rather

misleading.

Looking at Fig. 5 or 6 we may wonder why at $p_t \sim 2m_c$ the contribution from color octet ${}^3P_J$ and ${}^1S_0$ $c\bar{c}$ pairs exceeds the color singlet contribution by about a factor 20, although from the scaling rules the color octet contribution would have been expected to be suppressed by $v^4 \sim 1/10$. Since the ratio of matrix elements is indeed $M_{3.5}^{\psi}({}^1S_0^{(8)}, {}^3P_0^{(8)})/\langle \mathcal{O}_1^{\psi}({}^3S_1)\rangle \sim 4 \cdot 10^{-2}$, the short-distance coefficient of the octet term must be three orders of magnitudes larger than the coefficient of the singlet term. Examining the short-distance coefficients at $p_t = 2m_c$, one finds approximately

$$\frac{d\hat{\sigma}/dp_t^2[{}^3P_J^{(8)}]}{d\hat{\sigma}/dp_t^2[{}^3S_1^{(1)}]} \sim 81\,\frac{\hat{s}^2}{(2m_c)^4}, \tag{35}$$

where $\hat{s}$ is the partonic cms energy. The constant 81 is a large numerical factor, partly accidental, partly related to color factors and the larger number of P-wave intermediate states. The parametric ratio $\hat{s}^2/(2m_c)^4$ follows from the fact that diagrams with t-channel gluon exchange do not contribute to the leading order color singlet amplitude. Thus all propagators in the color singlet amplitude are off-shell by $\hat{s}$, while the octet amplitude is dominated by t-channel exchange that allows propagators to be off-shell by only $4m_c^2$. Because the gluon density favors small-x gluons, $\hat{s}$ is not tremendously large at the Tevatron. Nevertheless, at $p_t = 2m_c$, the lower kinematic limit specifies $\hat{s} \geq (1+\sqrt{2})^2\,(2m_c)^2 \sim 5.8\,(2m_c)^2$ and the ratio $\hat{s}^2/(2m_c)^4$ provides a further significant enhancement of the ampiltude. This rough estimate approximately coincides with the factor 10^3 estimated from Fig. 5.

It follows from this discussion that the next-to-leading α_s^4 color singlet contribution to which t-channel exchange diagrams contribute should be strongly enhanced as well and lead to large K-factors that increase with increasing transverse momentum, rather similar as in photoproduction.[39] At $p_t \gg 2m_c$, this contribution falls as $1/p_t^6$, slower as the lowest order contribution (but still faster than the fragmentation component (30)) and rather similar in shape to the ${}^3P_J$ and ${}^1S_0$ octet components. The value of $M_{3.5}^{\psi}({}^1S_0^{(8)}, {}^3P_0^{(8)})$ will therefore decrease to compensate for the additional singlet contribution.

Another source of potentially large higher-order corrections is related to initial state radiation. These, as does intrinsic transverse momentum, would primarily modify the p_t-distribution in the small-p_t region, up to at least several GeV. Initial state radiation could be treated either by analytic resummation or estimated

by Monte Carlo event generators. A first step in this direction has been taken.[40] The bulk effect seems to be an enhanced short-distance coefficient that leads to a decrease of both fitted color octet matrix elements. For a comparison of $\langle \mathcal{O}_8^\psi(^3S_1)\rangle$ in Ref.[40] and those quoted here and in Ref.[36] one has to take into account that the evolution of the fragmentation function in the $^3S_1^{(8)}$ channel has not been incorporated in Ref.[40]. Evolution depletes the fragmentation function at large z and consequently increases the fitted value of $\langle \mathcal{O}_8^\psi(^3S_1)\rangle$ by about a factor of 2.

3. Apart from higher-order radiative corrections, higher-order corrections in v^2, the parameter of the non-relativistic expansion, can be important close to boundaries of partonic thresholds, as discussed in Sect. 2.2. Such a situation occurs for the color octet fragmentation function that enters the most important fragmentation process (31) at large p_t. At the scale $2m_c$ it is given by[3]

$$D_{g\to\psi}(z,2m_c) = \frac{\pi\alpha_s(2m_c)}{24m_c^3}\,\delta(1-z)\,\langle \mathcal{O}_8^\psi(^3S_1)\rangle. \tag{36}$$

The delta-function clearly neglects that a fraction $\delta z \sim v^2$ of the gluon momentum is transferred to light hadrons in the 'hadronization' of the color octet intermediate state. Because of the steep p_t-distribution, negligence of this non-perturbative softening of the fragmentation function introduces a systematic bias[6,24,41] towards a too low fitted value of $\langle \mathcal{O}_8^\psi(^3S_1)\rangle$.

The momentum taken by the light degrees of freedom (light hadrons) is incorporated into the velocity expansion of NRQCD through operators with cms derivatives. Resumming the leading contribution results in[15]

$$D_{g\to\psi}(z,2m_c) = \frac{\pi\alpha_s(2m_c)}{24m_c^3}\int dy_+\,\delta(1-z-y_+)\,f_\psi[^3S_1^{(8)}](y_+), \tag{37}$$

where

$$\begin{aligned} f_\psi[^3S_1^{(8)}](y_+) \;&= \\ &\sum_{X,\lambda}\langle 0|\chi^\dagger\sigma^i T^a\psi|\psi(\lambda)+X\rangle\,\delta\Big(y_+ - [\Lambda\cdot(iD)]_+/k_+\Big)\,\langle\psi(\lambda)+X|\psi^\dagger\sigma^i T^a\chi|0\rangle. \end{aligned} \tag{38}$$

D denotes a (cms) derivative in the quarkonium rest frame, Λ the Lorentz boost that transforms it into a moving frame, '$+$' the light-cone 'plus'-component of a four-vector and k is the four-momentum of the 'hadronizing' color octet $c\bar{c}$ pair. The distribution $f_\psi[^3S_1^{(8)}](y_+)$ can be interpreted as a distribution of light-cone

momentum fraction y_+ taken by light hadrons in the process:[‡‡]

$$c\bar{c}[^3S_1^{(8)}] \to \psi + \text{light hadrons}. \tag{39}$$

After resummation the octet fragmentation function is expressed in terms of a new unknown function and all predictivity seems to be lost. However, we know that $f_\psi[^3S_1^{(8)}](y_+)$ should have support mainly in a region $y_+ \sim v^2$. Moreover, it is a universal function that could in principle be extracted from other processes not necessarily related to fragmentation. Once such a universal function is isolated, one can also try to model it and check the consistency of the ansatz in different production processes.

Summarizing this discussion, I think that regarding the numerical values of the matrix elements in (34) as accurate within a factor of 2 or less for $M_{3.5}^{\psi}({}^1S_0^{(8)}, {}^3P_0^{(8)})$ would not be overly conservative. It is worth noting that the color evaporation model mentioned earlier can reproduce the Tevatron data rather reasonably.[42] This is no surprize for the shape of the p_t-distribution, as the CEM includes a fragmentation component. It is less obvious that this works (again within factors of 2) with the same values of normalization factors f_ψ required to describe fixed-target data. From the point of view of NRQCD such agreement would be considered coincidental, perhaps related to the fact that the octet matrix elements relevant to both processes all scale equally as v^4.

Prompt S-wave bottomonium production has also been measured by CDF, although a χ_b-component could not yet be separated. A comparison with predictions can be found in Ref.[36]. As $v^4 \sim 1/100$ for bottomonium color octet contributions are less relevant than for charmonium in the region $p_t < 15\,\text{GeV}$ of the Tevatron data. Given the uncertainties in the color singlet contribution discussed above and the octet matrix elements for bottomonium, the necessity of color octet contributions is not yet as firmly established as for charmonium production. A realistic description of the p_t-spectrum requires the resummation of soft gluon radiation, which has not yet been undertaken.

[‡‡] While writing this review, I learnt of related ideas by M. Mangano, who introduces a similar distribution function on phenomenological grounds outside the context of the NRQCD expansion.

3.2 Polarization

Perhaps the most decisive test of the NRQCD picture of quarkonium production will come from a polarization measurement of direct J/ψ and ψ' at the Tevatron at large quarkonium transverse momentum. Recall that at large p_t, the production cross section is dominated by gluon fragmentation into $c\bar{c}[^3S_1^{(8)}]$. It was first noted by Cho and Wise[43] that the $c\bar{c}$ pair is transversely polarized, because the coupling of longitudinal gluons is suppressed by $4m_c^2/p_t^2$. Furthermore, to leading order in the velocity expansion the subsequent transition (39) takes place via a double electric dipole transition, which does not flip the heavy quark spin. Consequently, at large transverse momentum, one should observe transversely polarized quarkonia. The polarization can be observed in the angular distribution of decay leptons from $\psi \to l^+l^-$, which can be written as

$$\frac{d\Gamma}{d\cos\theta} \propto 1 + \alpha \cos^2\theta, \tag{40}$$

with θ the angle between the lepton three-momentum in the ψ rest frame and the polarization axis, the ψ direction in the hadronic cms frame (lab frame). Pure transverse polarization would imply $\alpha = 1$.

Corrections to the asymptotic limit come from three sources, corresponding to the three small parameters v^2, α_s/π and $4m_c^2/p_t^2$ that characterize quarkonium production at the Tevatron.* Since spin symmetry is violated by higher order interaction terms in the NRQCD Lagrangian, longitudinal polarization can arise if the transition (39) proceeds via two magnetic dipole transitions. These corrections scale as v^4 and do not vanish in the limit of large transverse momentum. According to the power counting estimate,[30] they could reduce α to 0.85.

The second source of corrections comes from α_s corrections to the fragmentation function, since radiation of a hard gluon can change the $c\bar{c}$ pair's polarization. This correction decreases with p_t as $1/(\ln p_t)$. All relevant fragmentation functions into longitudinally polarized quarkonia have been computed[30] and were found to yield about 5% longitudinal polarization at $p_t = 20\,\mathrm{GeV}$. The corrections turned out to be rather small, mainly because the fragmentation functions can only be softer than the leading term (36) that produces transverse charmonia. After convolution with the short-distance cross section this leads to suppression of the higher-order contribution. If added to the first correction, the

*I am ignoring higher-twist corrections which are suppressed in the small ratio Λ/p_t.

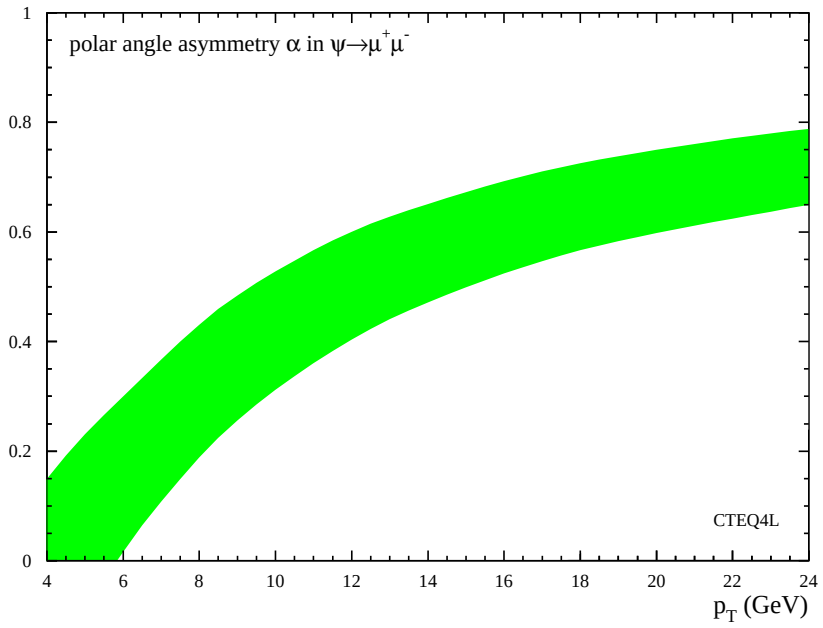

Figure 7: α as a function of p_t. Taken from Ref.[37].

second still implies that $\alpha > 0.65$ at $p_t = 20\,\text{GeV}$. This estimate is based on $\langle \mathcal{O}_8^\psi(^3P_0)\rangle/m_c^2 \approx \langle \mathcal{O}_8^\psi(^3S_1)\rangle$, consistent with Tab. 4 (CTEQ4L).

Below $p_t \sim 15\,\text{GeV}$ the dominant source of depolarization is due to non-fragmentation contributions,[37] because they have large short-distance coefficients as seen above. The size of these depends crucially on the magnitude of the parameter $M_{3.5}^\psi(^1S_0^{(8)},{}^3P_0^{(8)})$. With the value taken from Tab. 4, the prediction for the parameter α in the polar angle distribution is shown in Fig. 7. The band is based on the non-fragmentation corrections and α_s corrections to the fragmentation functions, but neglects the depolarization due to spin symmetry breaking of order $\delta\alpha \sim 0.1$. It is important that the band reflects only the uncertainties in the extraction of NRQCD matrix elements due to statistical errors in the data of the unpolarized cross section. It does not include any of the theoretical uncertainties that could systematically affect the extraction of these matrix elements. In particular, if $M_{3.5}^\psi(^1S_0^{(8)},{}^3P_0^{(8)})$ is smaller than assumed here, which is not unlikely, the transverse polarization fraction would increase. Nevertheless, at $p_t \sim 5\,\text{GeV}$, Fig. 7 shows that no remnant of transverse polarization may be expected. As p_t increases, the angular distribution becomes rapidly more anisotropic. If above $p_t \sim 20\,\text{GeV}$ a substantial fraction of transverse polarization is not observed in

future (run II) Tevatron data, we will definitely know that NRQCD, or at least spin symmetry, is not applicable at the charm mass scale. If it is observed, the color evaporation model will have lost most of its remaining appeal.

4 Quarkonium production at fixed target

It has long been known, and highlighted most recently in Refs.[20,44], that the color singlet model does not give a satisfactory description of all quarkonium production cross sections at fixed target energies. The discrepancies arise for direct J/ψ and χ_1, both of which can not be produced by gluon-gluon fusion at leading order in the color singlet channel. When the over-all normalization of the color singlet cross section is adjusted to the data, one also predicts a significant fraction of transverse polarization, $\alpha \approx 0.25$ in the notation of (40) and in the Gottfried-Jackson frame. No polarization is observed. As compared to the Tevatron 'ψ'-anomaly' these discrepancies are less dramatic and the theoretical uncertainties could always be stretched, and higher-twist effects invoked, to make them appear even less incisive. Nevertheless, these discrepancies must be reassessed in the light of the NRQCD factorization approach.

4.1 Cross sections

Fixed target quarkonium cross sections have been calculated by several collaborations.[31,45,46] The spin and color states that can be produced in parton-parton collisions at order α_s^2 are as follows:

$$\begin{aligned} gg &\to c\bar{c}[n]: \quad n = {}^1S_0^{(1,8)}, {}^3P_{0,2}^{(1,8)}, {}^1P_1^{(8)}, D\text{-waves}, \ldots \\ q\bar{q} &\to c\bar{c}[n]: \quad n = {}^3S_1^{(8)}, D\text{-waves}, \ldots . \end{aligned} \tag{41}$$

At order α_s^3, after hard gluon radiation, no stringent helicity and color constraints remain. Adopting a value for $\langle \mathcal{O}_8^{\psi}({}^3S_1)\rangle$ on the order of those shown in Tab. 4, the quark annihilation channel turns out to be insignificant at energies far enough from the $c\bar{c}$ threshold such that $x_1 x_2 \sim 4m_c^2/s \ll 1$ for the product of parton momentum fractions. The cross sections are then dominated by gluon-gluon fusion for both pion and proton beams. Keeping the intermediate $c\bar{c}$ states that are leading according to the scaling rules of Tab. 2, the direct J/ψ and ψ' production cross

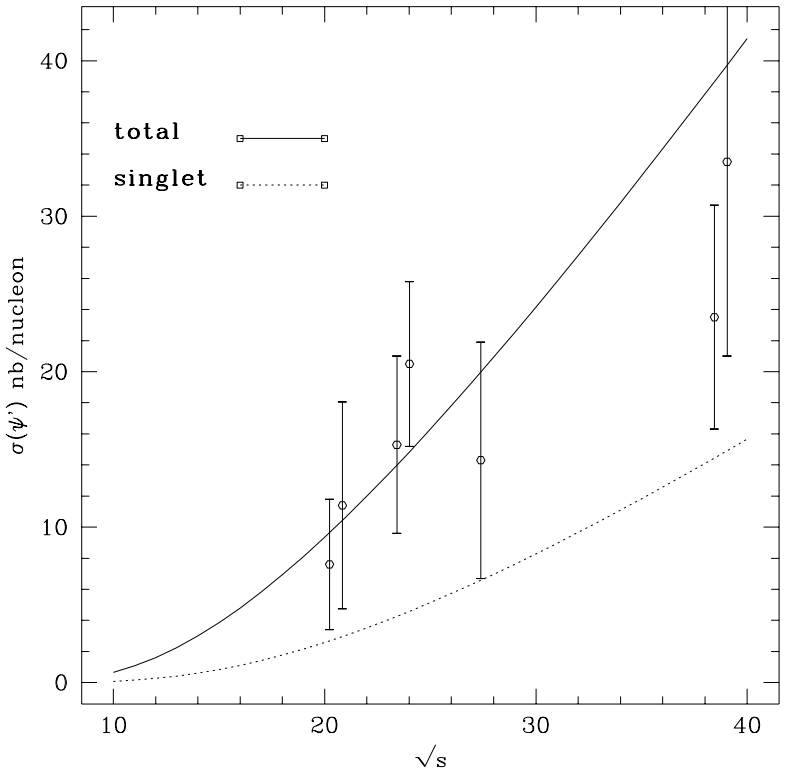

Figure 8: Total (solid) and singlet only (dotted) ψ' production cross section ($x_F > 0$) in proton-nucleon collisions. The solid line is obtained with $M_7^{\psi'}({}^1S_0^{(8)}, {}^3P_0^{(8)}) = 5.2 \cdot 10^{-3}\,\mathrm{GeV}^3$.

section is given by

$$\begin{aligned}
&\hat{\sigma}(gg \to \psi') \;\; = \\
&\frac{5\pi^3\alpha_s^2}{12(2m_c)^3 s}\,\delta\!\left(x_1x_2 - \frac{4m_c^2}{s}\right)\left[\langle\mathcal{O}_8^{\psi}({}^1S_0)\rangle + \frac{3}{m_c^2}\langle\mathcal{O}_8^{\psi}({}^3P_0)\rangle + \frac{4}{5m_c^2}\langle\mathcal{O}_8^{\psi}({}^3P_2)\rangle\right] \qquad (42)\\
&+\frac{20\pi^2\alpha_s^3}{81(2m_c)^5}\,\Theta\!\left(x_1x_2 - \frac{4m_c^2}{s}\right)\,\langle\mathcal{O}_1^{\psi}({}^3S_1)\rangle\, z^2\left[\frac{1-z^2+2z\ln z}{(1-z)^2} + \frac{1-z^2-2z\ln z}{(1+z)^3}\right],
\end{aligned}$$

where $z \equiv (2m_c)^2/(sx_1x_2)$, $\sqrt{s}$ is the center-of-mass energy and α_s is normalized at the scale $2m_c$. The third line gives the color singlet cross section that enters at order α_s^3. Using spin symmetry to relate $\langle\mathcal{O}_8^{\psi}({}^3P_J)\rangle = (2J+1)\,\langle\mathcal{O}_8^{\psi}({}^3P_0)\rangle$, the leading color octet contributions are proportional to $M_7^{\psi}({}^1S_0^{(8)}, {}^3P_0^{(8)})$ defined as in (33).

A comparison of the predicted energy dependence and normalization of the cross section (including the $q\bar{q}$ annihilation channel) with data is shown in Fig. 8

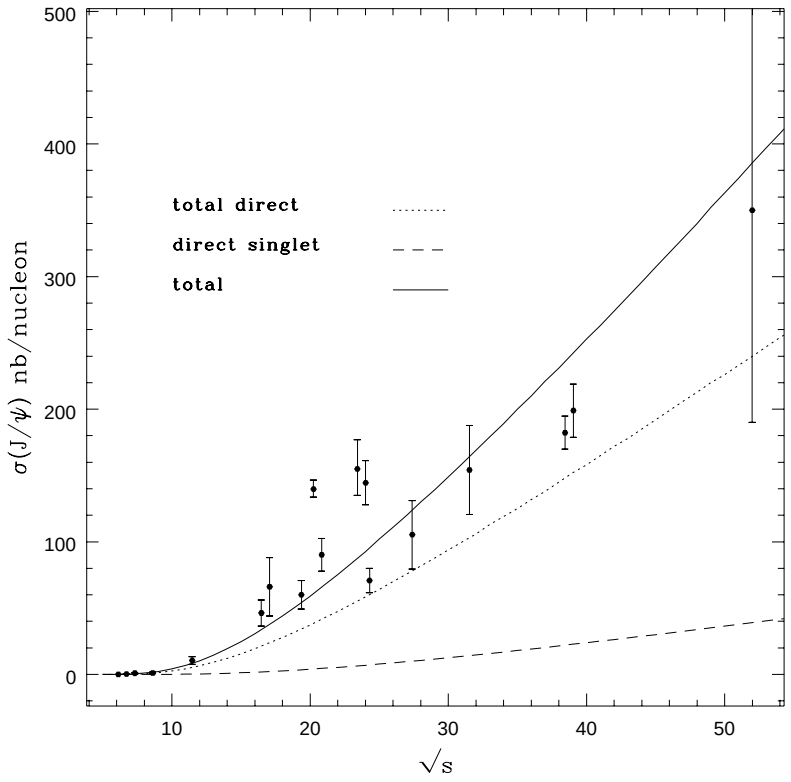

Figure 9: J/ψ production cross sections ($x_F > 0$) in proton-nucleon collisions. Solid line: Fit to the total cross section including radiative feed-down from the χ_{cJ} and ψ' with $M_7^{J/\psi}({}^1S_0^{(8)}, {}^3P_0^{(8)}) = 3.0 \cdot 10^{-2}\,\mathrm{GeV}^3$. Dashed line: Direct J/ψ cross section. Dotted line: Direct J/ψ production, color singlet only.

and 9 for ψ' and J/ψ production, respectively. The solid curves are obtained with

$$M_7^{\psi'}({}^1S_0^{(8)}, {}^3P_0^{(8)}) \equiv \langle \mathcal{O}_8^{\psi'}({}^1S_0)\rangle + \frac{7}{m_c^2}\langle \mathcal{O}_8^{\psi'}({}^3P_0)\rangle = 0.56 \cdot 10^{-2}\,\mathrm{GeV}^3$$
$$M_7^{J/\psi}({}^1S_0^{(8)}, {}^3P_0^{(8)}) \equiv \langle \mathcal{O}_8^{J/\psi}({}^1S_0)\rangle + \frac{7}{m_c^2}\langle \mathcal{O}_8^{J/\psi}({}^3P_0)\rangle = 3.0 \cdot 10^{-2}\,\mathrm{GeV}^3, \qquad (43)$$

with $m_c = 1.5\,\mathrm{GeV}$, which is assumed in this analysis. The color singlet contributions to the direct production cross section is shown separately. Note that since the $q\bar{q}$ annihilation channel is insignificant, the P-wave feed-down incorporated for J/ψ is entirely color singlet, because relativistic corrections to χ_1 production have been neglected. I will discuss χ production in more detail in Sect. 4.2.

Turning first to ψ' production, one notes that given the uncertainties inherent to leading order QCD predictions (no K-factors have been introduced), their

renormalization scale-dependence, as well as the dependence on m_c, the relevance of color octet contributions is far from obvious. This is mainly due to the fact that the color singlet cross section is dramatically enhanced compared to Ref.,[44] because it is expressed in terms of $2m_c = 3$ GeV rather than the significantly larger ψ' mass. Expressing the cross section in terms of quark masses implies a product $x_1 x_2$ smaller by 50% than its physical value and enhances the cross section as a consequence of the rising gluon density at small x. As noted earlier, this intrinsic ambiguity of a leading order calculation in v^2 would be alleviated by resumming higher-dimension operators. In the present case it is likely that the effect would be a reduction of the color singlet cross section, indicating more stringently a missing additional production mechanism. The short-distance coefficients of color octet production would be likewise affected by implementing the physical phase space constraints. In fact, as the invariant mass of the final state containing ψ' and light hadrons is even larger than $m_{\psi'}$, an even more significant reduction would be expected. A fit of the normalization to data would then require a larger $M_7^{\psi'}({}^1S_0^{(8)}, {}^3P_0^{(8)})$ than the one quoted in (43), which would be desirable in view of the apparent discrepancy between (43) and (34). Given these uncertainties, we can conclude that the sizes of color octet contributions as deduced from Tevatron and fixed target data are consistent with each other as far as order of magnitude is concerned and that one could not have hoped for more than that.

For J/ψ, Fig. 9, we have a clear deficit in the color singlet direct production cross section. The difference to ψ' comes from the fact that $m_{J/\psi}$ is not much larger than $2m_c$. While this does not remove the ambiguity with the choice of m_c, one would at least seem to be already closer to the physical phase space. If we assume that the P-wave feed-down is determined by leading order color singlet cross sections, an absolute prediction is obtained for the direct J/ψ cross section, once the unknown parameter $M_7^{J/\psi}({}^1S_0^{(8)}, {}^3P_0^{(8)})$ is fitted to the total J/ψ cross section. One finds that $\sigma(J/\psi)_{\rm dir}/\sigma(J/\psi) \approx 0.6$ in good agreement with experiment. On the other hand this ratio comes out a factor 3 too small with color singlet contributions only. The result $\sigma(J/\psi)_{\rm dir}/\sigma(J/\psi) \approx 0.6$ is still somewhat problematic, because it relies on the assumption that the χ feed-down is accurately reproduced and understood. But, as discussed in the following subsection, the χ_1/χ_2 composition of the χ feed-down assumed here conflicts with experiment in that there are too few χ_1 predicted. Thus there should be an additional, but neglected χ production mechanism that would then upset the nice agreement

found for $\sigma(J/\psi)_{\rm dir}/\sigma(J/\psi)$ (and make the color singlet model look even worse). This, however, can be compensated by taking into account the larger mass of χ states in the same way as for ψ'. Thus, it seems that color octet contributions in fixed target production are natural candidates to remove large discrepancies in over-all normalizations, but the remaining uncertainties preclude a straightforward test of the universality of color octet matrix elements by comparison with Tevatron data. In particular, one can not exclude the possibility of significant 'higher-twist' contributions that would have to be added on top of color octet contributions. The numerical situation will be considerably improved by the soon available next-to-leading QCD calculation of all relevant octet and singlet production channels. For P-waves this analysis has been reported in Ref.[24].

A comparison of cross sections in experiments with pion beams, using (43) extracted from proton beam experiments shows that the former are then systematically under-predicted by a factor of about 2. The resolution of this discrepancy, already known in the context of color singlet model predictions,[20] is clearly outside the scope of NRQCD, which assumes factorization of the hadronic initial from the hadronic final state.

The analysis of bottomonium S-wave cross sections suffers from the lack of sufficient experimental data, and in particular the absence of any experimental information on χ_b cross sections. Using color singlet wave functions and an estimate of color octet matrix elements, one finds[31] a larger indirect contribution to S-wave cross sections than for charmonium. The observation of $\Upsilon(3S)$ comparable to $\Upsilon(1S)$ in the E772 experiment[47] then indicates the existence of yet undetected $\chi_b(3P)$ states below the open bottom threshold.

In addition to integrated cross sections, x_F[48]and p_t[49] distributions may be analysed. Since the x_F distribution is determined by the gluon flux, the distributions are identical for color singlet and octet contributions and do not lead to further insight. Note that at large x_F the NRQCD expansion breaks down and higher-twist corrections become large.[50] A realistic comparison of p_t distributions in the range of available fixed target data requires yet accounting of soft gluon effects.

Experiment	beam/target	$\sqrt{s}$/GeV	R
E673	pBe	19.4/21.7	0.24 ± 0.28
E705	pLi	23.7	0.09
E771	pSi	38.8	0.34 ± 0.16
WA11	πBe	18.63	0.7 ± 0.2
E673	πBe	18.88	0.96 ± 0.64
E673	πBe	20.55	0.9 ± 0.4
E705	πLi	23.72	0.53
E672/706	πBe	31.08	0.57 ± 0.19

Table 5: Experimental data on the χ_1/χ_2 ratio R. Data compiled from Refs.[51]. In view of the experimental errors no attempt has been made to rescale older measurements to account for the latest χ branching fractions.

4.2 The χ_1/χ_2 ratio

As noted in (41), the leading-order gluon-gluon fusion process can not produce a spin-1 P-wave state. Consequently, at energies where $q\bar{q}$ annihilation is irrelevant,

$$R \equiv \frac{\sigma(\chi_1)}{\sigma(\chi_2)} = O\left(\frac{\alpha_s}{\pi}\right) \sim 0.05 \qquad \text{(color singlet)}, \tag{44}$$

with the numerical value from Ref.[31]. The data[51] compiled in Tab. 5 clearly show more copious χ_1 production.

In the context of the color singlet model, the χ_1 production cross section has sometimes been boosted by taking into account an exclusive quark-antiquark fusion mechanism[52] $q\bar{q} \to \chi_{cJ}$ at order α_s^4, see e.g. the cross sections displayed in Fig. 16 of Ref.[20]. As this mechanism produces χ_{cJ} states in the ratio 0:4:1, it raises R at low energies, especially in πN and $\bar{p}N$ collisions. The justification for keeping this higher-order contribution derives from the presence of two infrared logarithms, so that this contribution is of order $\alpha_s^4 \ln^2(m_c/\lambda)$, where $\ln(m_c/\lambda)$ is interpreted as a non-perturbative parameter. This bears some similarity with the infrared logarithm in $q\bar{q} \to \chi_{cJ} + g$ which, as discussed, could be interpreted as $q\bar{q} \to c\bar{c}[^3S_1^{(8)}] \to \chi_{cJ} + X$ in the framework of NRQCD factorization. This similarity is superficial, though, because the double logarithm above is not regularized by

the quarkonium binding energy and can not be absorbed into a NRQCD matrix element. Thus, if it existed, it would contradict NRQCD factorization. However, it seems clear that the origin of the double logarithm is the exclusive final state considered. The relevant cut diagram at order α_s^4 contains other cuts related to interfering $q\bar{q}g$ final states, which would cancel the infrared logarithms in agreement with NRQCD factorization. Thus, there is no infrared enhancement in the quark-antiquark fusion mechanism and it can not help to raise the χ_1/χ_2 ratio.

The next candidates are relativistic corrections in the velocity expansion.[31,53] Indeed, since they dominate direct J/ψ production, that suffers from the same suppression as χ_1 in the color singlet gluon-gluon fusion channel, they should naturally also be large for χ_1 production. The contributions that scale as v^4 relative to the leading order contribution for P-wave production are listed in Tab. 3. (In each channel, there exist v^2 corrections due to operators with spatial derivatives squared.) To get an estimate with no pretence of accuracy, let me consider only the octet ${}^3P_{J'}$ intermediate states. They yield

$$\frac{\sigma(\chi_1)\,\text{from}\,{}^3P_{J'}^{(8)}}{\sigma(\chi_2)\,\text{from}\,{}^3P_2^{(1)}} = \frac{15}{8}\,\frac{\langle\mathcal{O}_8^{\chi_1}({}^3P_2)\rangle + 15/4\langle\mathcal{O}_8^{\chi_1}({}^3P_0)\rangle}{\langle\mathcal{O}_1^{\chi_2}({}^3P_2)\rangle} \sim \frac{1}{3}, \tag{45}$$

where I assumed that $\langle\mathcal{O}_8^{\chi_1}({}^3P_2)\rangle/\langle\mathcal{O}_1^{\chi_2}({}^3P_2)\rangle \sim 1/10$ according to the scaling $v^4 \sim 1/10$. If we multiply this ratio by 2 to account for the intermediate S- and D-wave states, we obtain a χ_1 production cross section an order of magnitude larger than (44). Since the new production channels contribute also to χ_2 production, let me assume that they contribute to χ_1 and χ_2 in the ratio 3:5. Then

$$R \approx 0.3. \tag{46}$$

I emphasize again that this is a very crude estimate.[†] The estimate is in agreement with the χ_1/χ_2 ratio measured in pN collisions, but is lower than the measurement in πN collisions. If the trend of larger R for pion collisions exhibited by the measurements shown in Tab. 5 is confirmed, the real problem would no longer be the χ_1/χ_2 ratio per se, but the difference between proton and pion beam

[†] The short-distance coefficients of all v^4 suppressed intermediate states have recently been calculated.[54] Nevertheless, the significant number of new matrix element makes it difficult to improve on the crude estimate given here. The estimate of R given in Ref.[54] is larger than the one quoted here, because for unknown reasons the authors choose to omit the dominant color singlet channel in χ_2 production. Accounting for it makes their estimate consistent with (46).

experiments. Unless there is an unknown enhancement of the $q\bar{q}$ annihilation channel, such a difference would violate the initial/final state factorization of NRQCD and would have to be attributed to a 'higher-twist' effect. Note that as long as the $q\bar{q}$ annihilation channel can be neglected, the χ_1/χ_2 ratio should be approximately energy-independent.

4.3 Polarization

Polarization measurements have been performed for both ψ and ψ' production in pion scattering fixed target experiments.[55,56] Both experiments observe an essentially flat angular distribution in the decay $\psi \to \mu^+\mu^-$ ($\psi = J/\psi, \psi'$),

$$\frac{d\sigma}{d\cos\theta} \propto 1 + \alpha \cos^2\theta \,, \tag{47}$$

where the angle θ is defined as the angle between the three-momentum vector of the positively charged muon and the beam axis in the rest frame of the quarkonium. The observed values for α are 0.02 ± 0.14 for ψ', measured at $\sqrt{s} = 21.8$ GeV in the region $x_F > 0.25$ and 0.028 ± 0.004 for J/ψ measured at $\sqrt{s} = 15.3$ GeV in the region $x_F > 0$. In both cases the errors are statistical only.[‡]

Compared to these measurements, the color singlet contributions alone yield $\alpha \approx 0.25$ for the direct S-wave production cross section.[44] The polarization yield of octet contributions has been considered in Ref.[31].[§] The $c\bar{c}[^3S_1^{(8)}]$ intermediate state yields pure transverse polarization, but is insignificant for the total cross section, because it occurs only in $q\bar{q}$ annihilation. The $c\bar{c}[^1S_0^{(8)}]$ intermediate state results in unpolarized quarkonia while the $c\bar{c}[^3P_J^{(8)}]$ intermediate states prefer transverse to longitudinal polarization by a ratio 6:1. The longitudinal polarization fraction is therefore proportional to $M_3^\psi(^1S_0^{(8)}, ^3P_0^{(8)})$, different from the combination that enters the cross section summed over all polarizations. Constraining $\langle \mathcal{O}_8^\psi(^1S_0)\rangle$ and $\langle \mathcal{O}_8^\psi(^3P_0)\rangle$ to be positive, the range

$$0.15 < \alpha < 0.44 \tag{48}$$

[‡]Contemplating Fig. 11 of Ref.[55] I am strongly tempted to assume that the error is misprinted and that the measurement should read 0.028 ± 0.04.

[§]Polarization has also been treated in Ref.[45]. However, in the first reference of Ref.[45] and the preprint version of the second it was assumed that the $^1S_0^{(8)}$ production channel yields pure transverse polarization rather than no polarization, which leads to results significantly different from Ref.[31]. This has been corrected in the published version of the second reference.

is obtained for ψ' production at $\sqrt{s} = 21.8\,\mathrm{GeV}$. (The energy dependence is rather mild.) The lower bound is attained if $\langle \mathcal{O}_8^{\psi'}(^3P_0)\rangle = 0$ and could be as low as 0.08, since, as discussed in Sect. 4.1, the color singlet fraction in ψ' production is likely to be lower than that shown in Fig. 8. Thus, the prediction can be consistent with data within experimental errors, if $\langle \mathcal{O}_8^{\psi'}(^3P_0)\rangle$ is small compared to $\langle \mathcal{O}_8^{\psi'}(^1S_0)\rangle$. Such a scenario would be realized in case that the multipole suppression of $\langle \mathcal{O}_8^{\psi'}(^1S_0)\rangle$ is not effective ($\lambda \sim 1$ in Tab. 2).

The discussion for direct J/ψ production follows the ψ' case. To compare with the measurement, the polarization yield from χ and ψ' feed-down has to be computed. One then obtains

$$0.31 < \alpha < 0.62, \tag{49}$$

the larger value of α being related to the fact that only color singlet mechanisms to χ production were considered (so that the feed-down is almost purely χ_2, in conflict with experiment) and that χ_2 is produced only in a helicity ± 2 state in gluon-gluon fusion at leading order. The feed-down therefore yields an almost purely transversely polarized component to the J/ψ cross section. Eq. (49) is incompatible with the observed flat angular distribution. As a prediction it should however be taken with due caution. Taking the estimate of Sect. 4.2 literally, only one third of the χ feed-down is due to χ_2 produced in a color singlet state, while the polarization yield of the remainder is unknown. Thus, it does not seem excluded that the total χ feed-down is largely unpolarized, in which case α can be as small as 0.1. To resolve this issue, a measurement of χ polarization would be desirable. In particular, one would like to know to what extent χ_{c2} is produced with helicity ± 2. Meanwhile, the situation remains unclear and one may speculate on the role of higher-twist final state interactions without impunity.

The comparison with polarization data, as well as the compatibility of matrix elements determined from large-p_t and fixed target production, Eqs. (34) and (43) could be ameliorated, if, as has been suggested,[57] $\langle \mathcal{O}_8^{\psi}(^3P_0)\rangle$ is actually negative. This is indeed possible in principle for the renormalized matrix element, because of operator mixing, and in particular a quadratic divergence that would appear in schemes with an explicit factorization scale. However, phenomenologically, a negative value is unacceptable. The quadratic divergence implies that in any process $\langle \mathcal{O}_8^{\psi}(^3P_0)\rangle$ appears as a combination

$$\langle \mathcal{O}_8^{\psi}(^3P_0)\rangle + k\alpha_s\mu^2\langle \mathcal{O}_1^{\psi}(^3S_1)\rangle, \tag{50}$$

where μ denotes the factorization scale and the constant k follows from separating and including only the soft gluon contribution to the color singlet cross section. As this combination enters a physical cross section, it must be positive in any factorization scheme. On the other hand, in all phenomenological applications, the higher order color singlet piece is not included into the theoretical prediction or is argued to be smaller than the octet contribution. Consequently, the phenomenologically extracted value of $\langle \mathcal{O}_8^{\psi}(^3P_0)\rangle$ alone must satisfy the positivity constraint. If a fit prefers this matrix element to be negative, it must be attributed to uncertainties in either theory or data.

4.4 Beyond NRQCD

As emphasized in Sect. 2.2, the NRQCD factorization approach is leading twist and neglects potential interactions of the intermediate heavy quark pair with the beam or target remnants, as well as any production mechanism that involves multiparton interactions in the initial state. Quarkonium production cross sections in fixed target experiments, where most quarkonia escape at small angle with the beam axis, would be especially vulnerable to such corrections. In this subsection, I list some of such phenomena, that can not be described by NRQCD. For more comprehensive discussions and references, see the overviews given by Brodsky[58] and by Hoyer.[59]

Nuclear dependence. Charmonium production on nuclear targets shows suppression with increasing nucleon number, which is parametrized by $\sigma = \sigma_0\, A^{\alpha}$, where $\alpha \approx 0.9 - 0.92$ for cross sections integrated over positive x_F. Since $\alpha \approx 1$ for open charm production, this nuclear dependence can not be attributed to shadowing in parton distributions. NRQCD can not account for such a nuclear dependence due to rescattering of a $c\bar{c}$ pair with the nucleus. Since for bottomonia $\alpha \sim 0.97$, nuclear suppression is consistent with being higher twist. Note that in the nucleus rest frame, the charmonium formation time is long in a high energy collision and charmonium forms only after the $c\bar{c}$ pair has left the nucleus. Since most J/ψ are now believed to originate from a $c\bar{c}$ pair originally produced in a color octet state, the rescattering cross section is that of an octet rather a singlet $c\bar{c}$ pair. A further consequence is that despite their different sizes, the nuclear dependence should be the same for J/ψ and ψ' as is indeed observed.

Comover interactions. A $c\bar{c}$ pair that moves with nearly equal velocity as light quarks from the hadron remnants may find it preferable to produce open charm rather than charmonium. Comover interactions responsible for this effect would be expected to be largest in the nuclear fragmentation region ($x_F < 0$), because of the larger number of potential comovers. Consequently, α should decrease for $x_F < 0$, an effect that is observed for both charmonium and bottomonium.

Large-x_F phenomena. The region $x_F \to 1$ is particularly interesting, because the usual hard scattering picture breaks down in this region.[50] One way to visualize this is to note that all partons of the projectile have to be correlated in order that all momentum can be transferred to a single parton, that subsequently transfers all momentum of the projectile to the $c\bar{c}$ pair. Such a correlation is rather short-lived and at large x_F its lifetime can approach the hard interaction time scale set by $1/m_c$. A hard collision at large x_F then takes a snapshot of a compact Fock sate component of the projectile, for which multi-parton interactions are not suppressed. Such effects may explain the turn-over to longitudinal polarization at large x_F seen by the Chicago-Iowa-Princeton collaboration, and also a decrease of α towards 0.7 at large x_F, since the soft parton in the projectile stopped after transferring its momentum to the $c\bar{c}$ might then scatter only from the surface of the target nucleus. If the hadron wave function contains an intrinsic charm component (which it certainly does at some level), it would also naturally show itself at large x_F, as the intrinsic $c\bar{c}$ pair preferentially carries most of the projectile momentum. Charmonium production due to intrinsic charm is suppressed as Λ^2/m_c^2 (but can be sizeable in narrow kinematic regions) and is not included in NRQCD.

5 Conclusion

In this lecture I have tried to convey a topical overview on non-relativistic QCD as an effective theory and some of its applications. As any effective theory, NRQCD relies on the presence of different mass scales, here the quark mass m_Q and the quark's typical velocity $m_Q v$ and energy $m_Q v^2$ in a non-relativistic bound state. Assuming perturbation theory at the scale m_Q, NRQCD allows us to organize a calculation as an expansion in $\alpha_s(m_Q)$ and v^2. NRQCD shares many features with heavy quark effective theory and yet has a much richer structure owing to the existence of several low energy scales $m_Q v$, $m_Q v^2$ and Λ. As a consequence the

power counting in the effective theory is also complicated and one cannot rely on the dimension of operators alone. The velocity scaling rules of NRQCD are simple and unique in the Coulombic limit $m_Q v^2 \gg \Lambda$. If this limit were realized, our use of NRQCD would mimic non-relativistic QED and the bound state properties of quarkonia would be amenable to a perturbative treatment. As Λ is close to any of the two other bound state scales for charmonium, the velocity scaling is more delicate (and perhaps the most debated issue in NRQCD) and must in principle be assessed for every quarkonium state anew.

To describe quarkonium production, NRQCD has to be amalgamated with the concept of factorization in perturbative QCD. This opens tremendous perspectives on phenomenology, of which only a fraction could be reported here. New insights into quarkonium production followed from recognizing the importance of color octet and fragmentation production mechanisms, both of which are crucial in accounting for the charmonium cross sections observed in the Fermilab Tevatron experiments.

Nevertheless, NRQCD is not a 'Theory of Everything' in quarkonium production. The factorization formula for quarkonium production can be compared to the factorization theorem for Drell-Yan processes, with higher twist corrections due to, for example, initial and final state multi-parton interactions neglected in both cases. Such corrections may be more or less severe dependent on the production process, but would affect fixed target and forward photoproduction in particular. The comparison of leading twist predictions with fixed target data showed significant improvement in all aspects compared to the color singlet model, although some features such as χ production and ψ polarization could be made just consistent with data only upon straining the theory to its limits, which does not appear entirely satisfactory. In any case, even without higher twist corrections, theoretical uncertainties remain appreciable and complicate a verification of the universality of long-distance matrix elements in NRQCD. It seems, at least in my opinion, that at this moment there is no discrepancy in any process, including those not discussed here, that could not be attributed to one or another difficulty in the theoretical prediction, and which thus is understood, even if it is not easily remedied. As concerns fixed target experiments, much clarity could be obtained from measurements of χ polarization, polarization of $\Upsilon(nS)$ and separate χ_b cross sections.

For any theory, the question 'Can it be wrong?' is at least as important as

'Is it correct?'. Since, in the asymptotic limit $m_Q \to \infty$, NRQCD is evidently as correct as QCD itself, one should ask whether it could generally be inapplicable at the charmonium scale. Here, at last, the situation is clear: ψ' or direct J/ψ polarization at the Tevatron at large transverse momentum will evidence dramatic success or failure of NRQCD for charmonium production.

Acknowledgements. I wish to thank Michael Krämer and Ira Rothstein for their collaboration on quarkonia and Gerhard Schuler for many discussions and careful reading of the manuscript.

References

[1] J.J. Aubert *et al.*, Phys. Rev. Lett. **33** (1974) 1404; J.-E. Augustin *et al.*, Phys. Rev. Lett. **33** (1974) 1406.

[2] G.T. Bodwin, E. Braaten and G.P. Lepage, Phys. Rev. **D51** (1995) 1125.

[3] E. Braaten and S. Fleming, Phys. Rev. Lett. **74** (1995) 3327.

[4] F. Abe *et al.*, Phys. Rev. Lett. **69** (1992) 3704.

[5] E. Braaten, S. Fleming and T.C. Yuan, Ann. Rev. Nucl. Part. Sci. **46** (1996) 197.

[6] M. Beneke, in 'Proceedings of the Second Workshop on Continuous Advances in QCD', Minneapolis, M. Polikarpov (ed.), World Scientific, Singapore, 1996, p. 12 [hep-ph/9605462]

[7] A comprehensive overview as of summer 1996 can be found in the Proceedings of the Quarkonium Physics Workshop, University of Illinois, Chicago, June 1996.

[8] W.E. Caswell and G.P. Lepage, Phys. Lett. **B167** (1986) 437.

[9] T. Kinoshita and M. Nio, Phys. Rev. **D53** (1996) 4909; M. Nio and T. Kinoshita, CLNS97/1463 [hep-ph/9702218].

[10] J.G. Körner and G. Thompson, Phys. Lett. **B264** (1991) 185; S. Balk, J.G. Körner and D. Pirjol, Nucl. Phys. **B428** (1994) 499.

[11] E. Eichten and B. Hill, Phys. Lett. **234** (1990) 511; B. Grinstein, Nucl. Phys. **B339** (1990) 253; H. Georgi, Phys. Lett. **B240** (1990) 253.

[12] E. Eichten *et al.*, Phys. Rev. **D17** (1977) 3090.

[13] E. Braaten and Y.-Q. Chen, Phys. Rev. **D54** (1996) 3216.

[14] T. Mannel and G.A. Schuler, Z. Phys. **C67** (1995) 159.

[15] M. Beneke, I.Z. Rothstein and M.B. Wise, in preparation.

[16] T. Mannel and S. Wolf, TTP 97-02 [hep-ph/9701324].

[17] I.Z. Rothstein and M.B. Wise, UCSD-97-02 [hep-ph/9702404].

[18] R. Barbieri *et al.*, Phys. Lett. **B95** (1980) 43; Nucl. Phys. **B192** (1981) 61.

[19] G.T. Bodwin, E. Braaten and G.P. Lepage, Phys. Rev. **D46** (1992) 1914.

[20] G.A. Schuler, 'Quarkonium production and decays', CERN-TH-7170-94 [hep-ph/9403387].

[21] C.-H. Chang, Nucl. Phys. **B172** (1980) 425, E.L. Berger and D. Jones, Phys. Rev. **D23** (1981) 1521, R. Baier and R. Rückl, Phys. Lett. **B102** (1981) 364 and Ref.[20] for a review.

[22] A.V. Manohar, UCSD/PTH 97-01 [hep-ph/9701294].

[23] B. Grinstein and I.Z. Rothstein, UCSD-97-06 [hep-ph/9703298].

[24] M. Mangano and A. Petrelli, CERN-96-293 [hep-ph/9610364], to appear in the Proceedings of the Quarkonium Physics Workshop, University of Illinois, Chicago, June 1996.

[25] G.P. Lepage *et al.*, Phys. Rev. **D46** (1992) 4052

[26] P. Labelle, McGill/96-33 [hep-ph/9608491].

[27] G.T. Bodwin, E. Braaten and G.P. Lepage, erratum to Ref.[2], January 1997.

[28] G.A. Schuler, CERN-TH/97-12 [hep-ph/9702230], to appear in the Proceedings of the Quarkonium Physics Workshop, University of Illinois, Chicago, June 1996.

[29] H. Fritzsch, Phys. Lett. **B67** (1977) 217; F. Halzen, Phys. Lett. **B69** (1977) 105.

[30] M. Beneke and I.Z. Rothstein, Phys. Lett. **B372** (1996) 157 [Erratum: *ibid.* **B389** (1996) 789].

[31] M. Beneke and I.Z. Rothstein, Phys. Rev. **D54** (1996) 2005 [Erratum: *ibid.* **D54** (1996) 7082]; I.Z. Rothstein, UCSD-96-22 [hep-ph/9609281], to appear in the Proceedings of the Quarkonium Physics Workshop, University of Illinois, Chicago, June 1996.

[32] M.W. Bailey (for the CDF coll.), FERMILAB-CONF-96-235-E; A. Sansoni (for the CDF coll.), FERMILAB-CONF-96-221-E; V. Papdimitriou (for the CDF coll.), to appear in the Proceedings of the Quarkonium Physics Workshop, University of Illinois, Chicago, June 1996.

[33] E. Braaten and T.C. Yuan, Phys. Rev. Lett. **71** (1993) 1671.

[34] M. Cacciari and M. Greco, Phys. Rev. Lett. **73** (1994) 1586; E. Braaten, M. Doncheski, S. Fleming and M. Mangano, Phys. Lett. **B333** (1994) 548; D.P. Roy and K. Sridhar, Phys. Lett. **B339** (1994) 141.

[35] M. Cacciari, M. Greco, M.L. Mangano and A. Petrelli, Phys. Lett. **B356** (1995) 560.

[36] P. Cho and A.K. Leibovich, Phys. Rev. **D53** (1996) 150; **D53** (1996) 6203.

[37] M. Beneke and M. Krämer, CERN-96-310 [hep-ph/9611218], to appear in Phys. Rev. **D**.

[38] M. Glück, E. Reya and A. Vogt, Z. Phys. **C67** (1995) 433; A.D. Martin, R.G. Roberts and W.J. Stirling, Phys. Lett. **387** (1996) 419; H.L. Lai *et al.*, Phys. Rev. **D55** (1997) 1280.

[39] M. Krämer, Nucl. Phys. **B459** (1996) 3.

[40] B. Cano-Coloma and M.A. Sanchis-Lozano, IFIC/97-1 [hep-ph/9701210].

[41] P. Ernström, L. Lönnblad and M. Vänttinen, NORDITA-96-78-P [hep-ph/9612408].

[42] J. Amundson *et al.*, Phys. Lett. **390** (1997) 323; G.A. Schuler and R. Vogt, Phys. Lett. **B387** (1996) 181.

[43] P. Cho and M.B. Wise, Phys. Lett **B346** (1995) 129.

[44] M. Vänttinen, P. Hoyer, S.J. Brodsky and W.-K. Tang, Phys. Rev. **D51** (1995) 3332.

[45] W.-K. Tang and M. Vänttinen, Phys. Rev. **D53** (1996) 6203; Phys. Rev. **D54** (1996) 4349.

[46] S. Gupta and K. Sridhar, Phys. Rev. **D54** (1996) 5545.

[47] D.M. Alde *et al.*, Phys. Rev. Lett. **66** (1991) 2285

[48] S. Gupta and K. Sridhar, Phys. Rev. **D55** (1997) 2650.

[49] L. Slepchenko and A. Tkabladze, contribution to the 3rd German-Russian Workshop on Progress in Heavy Quark Physics, Dubna, Russia, May 1996 [hep-ph/9608296].

[50] S.J. Brodsky *et al.*, Nucl. Phys. **B369** (1992) 519.

[51] Y. Lemoigne *et al.*, Phys. Lett. **B113** (1982) 509; S.R. Hahn *et al.*, Phys. Rev. **D30** (1984) 671; D.A. Bauer *et al.*, Phys. Rev. Lett. **54** (1985) 753; L. Antoniazzi *et al.*, Phys. Rev. **D49** (1994) 543; V. Koreshev *et al.*, Phys. Rev. Lett. **77** (1996) 4294; K. Hagan (for the E771 collaboration), to appear in the Proceedings of the Quarkonium Physics Workshop, University of Illinois, Chicago, June 1996.

[52] J.H. Kühn, Phys. Lett. **B89** (1980) 385.

[53] S. Gupta and P. Mathews, TIFR/TH/96-53 [hep-ph/9609504], to appear in Phys. Rev. **D**.

[54] S. Gupta and P. Mathews, TIFR/TH/97-08 [hep-ph/9703370].

[55] C. Akerlof *et al.*, Phys. Rev. **D48** (1993) 5067.

[56] J.G. Heinrich *et al.*, Phys. Rev. **D44** (1991) 1909.

[57] S. Fleming *et al.*, Phys. Rev. **D55** (1997) 4098.

[58] S.J. Brodsky, SLAC-PUB-7306 [hep-ph/9609415], to appear in the Proceedings of the Quarkonium Physics Workshop, University of Illinois, Chicago, June 1996.

[59] P. Hoyer, NORDITA-97-8-P [hep-ph/9702385], talk given at the 2nd ELFE Workshop, St. Malo, France, September 1996.